Site-specific Inhibitory Mechanism for Amyloid-β42 Aggregation by Catechol-Type Flavonoids Targeting the Lys Residues*

Mizuho Sato[1†], Kazuma Murakami[1], Mayumi Uno[1], Yu Nakagawa[1,2], Sumie Katayama[3], Ken-ichi Akagi[3], Yuichi Masuda[4,5], Kiyonori Takegoshi[4], and Kazuhiro Irie[1]

From [1]Division of Food Science and Biotechnology, Graduate School of Agriculture, Kyoto University, Kyoto 606-8502, Japan
[2]Synthetic Cellular Chemistry Laboratory, RIKEN Advanced Science Institute, Saitama 351-0198, Japan
[3]National Institute of Biomedical Innovation, Osaka 567-0085, Japan
[4]Department of Chemistry, Graduate School of Science, Kyoto University, Kyoto 606-8502, Japan
[5]Graduate School of Pharmaceutical Sciences, Tohoku University, Sendai 980-8578, Japan

*Running title: *Inhibitory Mechanism of Aβ42 Aggregation by Flavonoids*

To whom correspondence should be addressed: Kazuhiro Irie, Ph.D., Kitashirakawa Oiwake-cho, Sakyo-ku, Kyoto 606-8502, Japan. Tel.: +81-75-753-6281, Fax: +81-75-753-6284, E-mail: irie@kais.kyoto-u.ac.jp
Keywords: Alzheimer's disease, amyloid β, aggregation, flavonoid, catechol

Background: The inhibitory mechanism of Aβ42 aggregation by flavonoid is fully unknown.
Results: The oxidant enhanced the inhibitory activity of (+)-taxifolin against Aβ42 aggregation by forming Aβ42-taxifolin adducts between the Lys-residues and oxidized (+)-taxifolin.
Conclusion: The inhibitory activity of catechol-type flavonoids requires auto-oxidation to form an *o*-quinone to react with Lys.
Significance: These may help design promising inhibitors against Aβ42 aggregation for Alzheimer's therapy. (60<60 words)

SUMMARY (239<250 words)

The aggregation of 42-residue amyloid β-protein (Aβ42) is involved in the pathogenesis of Alzheimer's disease (AD). Numerous flavonoids exhibit inhibitory activity against Aβ42 aggregation, but their mechanism remains unclear in molecular level. Here we propose the site-specific inhibitory mechanism of (+)-taxifolin, a catechol-type flavonoid, whose 3',4'-dihydroxyl groups of the B-ring plays a critical role. Addition of sodium periodate, an oxidant, strengthened suppression of Aβ42 aggregation by (+)-taxifolin, whereas no inhibition was observed under anaerobic conditions, suggesting the inhibition to be associated with the oxidation to form *o*-quinone. Since the formation of Aβ42-taxifolin adduct was suggested by mass spectrometry, Aβ42 mutants substituted at Arg5, Lys16, and/or Lys28 with norleucine (*n*L) were prepared to identify the residues involved in the conjugate formation. (+)-Taxifolin did not suppress the aggregation of Aβ42 mutants at Lys16 and/or Lys28 except for the mutant at Arg5. In addition, the aggregation of Aβ42 was inhibited by other catechol-type flavonoids, while that of K16*n*L-Aβ42 was not. In contrast, some non-catechol-type flavonoids suppressed the aggregation of K16*n*L-Aβ42 as well as Aβ42. Furthermore, interaction of (+)-taxifolin with β-sheet region in Aβ42 was not observed using solid-state NMR unlike curcumin of non-catechol-type. These results demonstrate that catechol-type flavonoids could specifically suppress Aβ42 aggregation by targeting Lys-residues. Although the anti-AD activity of flavonoids has been ascribed to their anti-oxidative activity, the mechanism that the *o*-quinone reacts with Lys-residues of Aβ42 might be more intrinsic. The Lys-residues could be targets for Alzheimer's therapy.

Alzheimer's disease (AD) is characterized by amyloid deposition in senile plaques mainly consisting of 40- and 42-mer amyloid β-proteins (Aβ40, Aβ42) (1,2). These proteins are generated from the amyloid precursor protein by β- and γ-secretases (amyloidogenic pathway). Aβ aggregates mainly through intermolecular β-sheet formation and shows neurotoxicity *in vitro* (3). Aβ42 plays a more pivotal role in the pathogenesis of AD than Aβ40 because of its higher aggregative ability and neurotoxicity (3). It has been well documented that soluble Aβ oligomeric assemblies rather than insoluble fibrils cause memory loss and neuronal death (4,5). Oxidative stress is one of the major contributing factors to neurodegenerative disease progression (6). Aβ-induced toxicity has been correlated to oxidative damage through protein radicalization *in vitro* (7,8) and *in vivo* (9,10).

Researchers have reported protective effects of various polyphenols from green tea, turmeric, and red wine *etc*., against Aβ aggregation and neurotoxicity (11-13). Several compounds [e.g. (-)-epigallocatechin-3-gallate (EGCG), curcumin, and resveratorol] are in clinical or preclinical trials for AD treatment (14,15). However, the recent failures of some trials (16) motivated us to clarify the mechanism by which polyphenols inhibit the aggregation of Aβ42 to develop promising leads for clinical use.

Concerning the molecular interaction of Aβ with flavonoids, a docking simulation by Keshet *et al*. predicted the involvement of Lys28 and the C-terminal region in the binding with myricetin (17). However, the precise mode of binding with flavonoids has scarcely been addressed, except for limited studies using NMR spectroscopy [curcumin (18), EGCG (19), and myricetin (20)], which suggested less-specific interaction with the β-sheet region in Aβ.

Our group recently found that silymarin, seed extracts of *Silybum marianum*, attenuated AD-like pathologic features, such as senile plaques, neuroinflammation, behavioral dysfunction, and Aβ oligomer formation using a well-established AD mouse model (J20) (21). We also isolated (+)-taxifolin (22), a flavanonol which has a catechol moiety on the B-ring (Fig. 1A), as a component of the extracts that prevents Aβ42 aggregation (23). "Aggregation" used in this paper means the process of Aβ42 monomer to form fibrils by way of oligomer and/or protofibril. This paper describes a comprehensive study on the ability of (+)-taxifolin to prevent aggregation and β-sheet formation of Aβ42, along with the effects of various flavanonols and flavonols on the aggregation of Aβ42 mutants substituted at Arg5, Lys16, and/or Lys28 with norleucine (*n*L). These results together with the results of liquid chromatography-mass spectrometry (LC-MS) led us to propose a site-specific inhibitory mechanism for Aβ42 aggregation by catechol-type flavonoids, where adduct formation at the Lys-residues in Aβ42 with the *o*-quione derived from flavonoids could be involved in the suppression of Aβ42 aggregation.

EXPERIMENTAL PROCEDURES

Synthesis of (+)-Taxifolin, Dihydrokaempferol and Pinobanksin— A naturally-occurring form of (+)-taxifolin was synthesized (Scheme S1A in Supplemental Data) basically according to the previous reports (23,24). Briefly, vanillin was demethylated by treatment with boron tribromide to give 3,4-dihydroxybenzaldehyde quantitatively, whose phenolic hydroxyl groups were protected with methoxymethyl groups. The phenolic hydroxyl groups of 2,4,6-trihydroxyacetophenone were also protected with methoxymethyl groups. A cross-aldol reaction between these products, followed by treatment with H_2O_2 under a basic condition, yielded the epoxide **7** (supplemental Scheme S1A), which was cyclized and deprotected under an acidic condition to give (±)-taxifolin. (+)-Taxifolin was separated by HPLC on a CHIRALCEL OJ-RH column (10 mm i.d. x 150 mm; Daicel Corporation, Osaka, Japan) using 15% CH_3CN/H_2O containing 0.1 % acetic acid (25). Synthesis of $^{13}C_6$-(+)-taxifolin was performed by using vanillin-ring-$^{13}C_6$ (Isotec, Miamisburg, OH) as a starting material.

(±)-Dihydrokaempferol (26) and (±)-pinobanksin (27) were synthesized in a manner similar to (±)-taxifolin using 4-hydroxybenzaldehyde or benzaldehyde in place of vanillin as a starting material, respectively

(supplemental Scheme S1A). Enantiomers were not separated because the inhibitory effect on Aβ42 aggregation by (–)-taxifolin was almost the same as that by (+)-taxifolin (23). The structure of each of these compounds was confirmed by ^{1}H NMR (AVANCE III 500, ref. TMS, Bruker, Germany) and EI-MS (JMS-600H, JEOL, Tokyo, Japan). EI-MS data were as follows: (+)-taxifolin (*m/z* 304 $[M]^{+}$), $^{13}C_6$-(+)-taxifolin (*m/z* 310 $[M]^{+}$), dihydrokaempferol (*m/z* 288 $[M]^{+}$), and pinobanksin (*m/z* 272 $[M]^{+}$). The spectra of ^{1}H NMR (28) and ^{13}C NMR (29) of $^{13}C_6$-(+)-taxifolin are shown in supplemental Fig. S1. The optical rotation of each enantiomer was; (+)-taxifolin $[\alpha]_D$ +17.3 (*c* 0.1, MeOH), (–)-taxifolin $[\alpha]_D$ –16.2 (*c* 0.1, MeOH), almost equal to those reported previously; (+)-taxifolin $[\alpha]_D$ +19.0 (*c* 0.1, MeOH) (22). Other flavonoids; myricetin (Wako, Osaka, Japan), kaempferol, (±)-dihydromyricetin (ChromaDex, Irvine, CA), morin, galangin, quercetin (Sigma, St. Louis, MO), and datiscetin (Extrasynthese, Genay, France) were purchased commercially.

Trapping of the o-*Quinone Form of (+)-Taxifolin by Phenylenediamine*—Sodium periodate ($NaIO_4$, 19 mg, 89 μmol) in H_2O (0.20 mL) was added to (±)-taxifolin (28 mg, 91 μmol; Toronto Research Chemicals Inc. North York, ON, Canada) in methanol (3.5 mL). After stirring for 15 min at room temperature, the reaction mixture was extracted with ethyl acetate (5.0 mL), to which 1,2-phenylenediamine (9.8 mg, 91 μmol; Wako) was added before stirring for 30 min at room temperature. The mixture was concentrated and separated by HPLC on a YMC SH-342-5AL column (20 mm i.d. x 150 mm; YMC, Kyoto, Japan) with 60% MeOH/H_2O to give the corresponding phenazine (3.8%) (supplemental Scheme S1B). The structure was confirmed by ^{1}H NMR and high resolution (HR)-EI-MS. ^{1}H NMR (500 MHz, 295.3 K, acetone-d_6, 6.98 mM) δ 4.87 (1H, d, J = 11.5 Hz), 5.59 (1H, d, J = 11.5 Hz), 6.07 (1H, s), 6.09 (1H, s), 7.96-8.00 (2H, m), 8.22 (1H, dd, J = 9.0, 1.7 Hz), 8.26-8.30 (2H, m), 8.33 (1H, d, J = 9.0 Hz), 8.46 (1H, d, J = 1.7 Hz), 11.72 (1H, brs); HR-EI-MS *m/z* 374.0902 $[M]^{+}$, calcd for $C_{21}H_{14}N_2O_5$ 374.0903.

Thioflavin-T Fluorescence Assay—The aggregative ability of Aβ42 was evaluated at 37 °C by the thioflavin-T (Th-T) method developed by Naiki *et al* (30). The procedure was described elsewhere (31). Fluorescence intensity was measured at 420 nm excitation and 485 nm emission using a micro-plate reader (MPR-A4ιII; TOSOH, Tokyo, Japan, or Fluoroskan Ascent; Thermo Scientific, Rockford, IL). In brief, Aβ42 was dissolved in 0.1% NH_4OH at 250 μM, and each flavonoid was dissolved in EtOH at 5 mM, followed by dilution with sodium phosphate-buffered saline (PBS: 50 mM sodium phosphate and 100 mM NaCl, pH 7.4) at the desired concentration (Aβ42, 25 μM; flavonoids, 50 μM). $NaIO_4$ or Tris(2-carboxyethyl)phosphine hydrochloride (TCEP-HCl) was initially dissolved in PBS at 100 mM, then diluted with PBS at 100 μM before use. Experiments under an anaerobic condition were performed in a desiccator evacuated by a diaphragm pump (*ca*. 8 mmHg; KNF Lab LABOPORT vacuum pump, KNF Neuberger, NJ) at room temperature. Unless otherwise noted, the concentrations of Aβ42, flavonoids, and oxidant/reductant used in this study were 25, 50, and 100 μM, respectively.

The effect of the addition of $NaIO_4$ on Met35 oxidation was estimated by HPLC on a Develosil ODS UG-5 column (6.0 mm i.d. x 100 mm; Nomura chemical, Seto, Japan) under a gradient of 10-50% CH_3CN containing 0.1% NH_4OH for 40 min after the centrifugation of the Aβ42 solution at 20,130 *g* at 4 °C (MX-300; TOMY, Tokyo, Japan) for 10 min.

The seeds of Aβ42 were also prepared basically according to the protocol developed by Naiki *et al* (30). Briefly, after incubation of Aβ42 (25 μM) in PBS (pH 7.4) for 24 h at 37 °C, the pellet obtained by centrifugation at 20,130 *g* at 4 °C for 1 h was suspended by pipetting in PBS (pH 7.4) at concentration of 1 mg/mL. The resultant solution was sonicated for 1 h in an ultrasonic device (MUS-20; EYELA, Tokyo, Japan), followed by dilution with PBS at 10 μg/mL before use. Th-T relative fluorescence was expressed as a percentage of wild-type Aβ42

alone, whose maximum value was taken as 100%.

Transmission Electron Microscopy (TEM)—The aggregates of Aβ42 after a 48-h incubation were examined under a H-7650 electron microscope (Hitachi, Ibaraki, Japan). The experimental procedure was described elsewhere (31).

UV-visible Spectrometry—Oxidation of (+)-taxifolin was monitored by UV spectroscopy (UV-2200A; Shimadzu, Kyoto, Japan). (+)-Taxifolin (50 μM) was incubated with Aβ42 (25 μM) in PBS (50 mM sodium phosphate and 100 mM NaCl, pH 7.4) at 37 ^{o}C. The solution was then loaded into a 1-cm path length quartz cell, and UV spectra were recorded at 200-500 nm. The sample was diluted three times with PBS because of its strong absorbance.

Circular Dichroism (CD) Spectrometry—The secondary structure of Aβ42 was estimated by CD spectrometry (J-805; JASCO, Tokyo, Japan) using a 0.1-mm quartz cell (121.027-QS, ϕ 10 mm; JASCO), as described elsewhere (32). Aβ42 (25 μM) was incubated with or without (+)-taxifolin (50 μM) in PBS (50 mM sodium phosphate and 100 mM NaCl, pH 7.4) at 37 ^{o}C. An aliquot was loaded into the quartz cell, and CD spectra were recorded at 190-250 nm. Experiments under an anaerobic condition were performed as described before. The spectra of Aβ42 mutants are shown after subtraction of the spectrum for vehicle alone, and those in the presence of (+)-taxifolin are shown after subtraction of the spectrum for (+)-taxifolin alone.

LC-MS Analysis—Aβ42 solution (25 μM) was incubated with 50 μM (+)-taxifolin in PBS (50 mM sodium phosphate and 100 mM NaCl, pH 7.4) in the presence of 100 μM $NaIO_4$ at 37 ^{o}C. After a 4-h incubation, the mixture was desalted and condensed twice by ZipTip C18 (Millipore, Bedford, MA). Five microliters of the solution was subjected to a liquid chromatography mass spectrometry ion trap time-of-flight (LCMS-IT-TOF; Shimadzu) through a YMC-Pack ODS-AQ column (6.0 mm i.d. x 100 mm; YMC) at 25 ^{o}C under a gradient of 20-60% CH_3CN containing 0.1% formic acid for 30 min.

Synthesis of Aβ42 Mutants—Fmoc-norleucine (*n*L)-OH was purchased from Watanabe Chemical Industries (Hiroshima, Japan). L-Alanine ($^{13}C_3$, ^{15}N), L-phenylalanine ($^{13}C_{\beta}$), and L-valine ($^{13}C_5$, ^{15}N) were purchased from Isotec, and L-lysine ($^{13}C_6$, $^{15}N_2$) and L-serine ($^{13}C_3$, ^{15}N) from Cambridge Isotope Laboratories (Frontage Road Andover, MA). Each labeled amino acid was protected by an Fmoc group as previously reported (33,34). The structure of each Fmoc derivative was confirmed by ^{1}H NMR, ^{13}C NMR, and FAB-MS.

The Aβ42 mutants were synthesized in a stepwise fashion on 0.1 mmol of preloaded Fmoc-L-Ala-PEG-PS resin using a Pioneer™ Peptide Synthesizer (Applied Biosystems, Foster City, CA) as reported previously (35). After the chain elongation was completed, the peptide-resin was treated with a cocktail containing trifluoroacetic acid, *m*-cresol, thioanisol, and 1,2-ethanedithiol for final deprotection and cleavage from the resin. The crude peptide was precipitated by diethylether and purified by HPLC under an alkaline condition as described previously (31). After lyophilization, we obtained the corresponding pure Aβ42 peptide, the purity of which was confirmed by HPLC (>98%). The molecular weight of each Aβ42 mutant was confirmed by matrix-assisted laser desorption/ionization time-of-flight mass spectrometry (MALDI-TOF-MS, AXIMA-CFR; Shimadzu); R5*n*L-Aβ42 (*m/z*, calcd: 4472.11, found: 4472.38 $[M+H]^+$), K16*n*L-Aβ42 (*m/z*, calcd: 4500.12, found: 4500.25 $[M+H]^+$), K28*n*L-Aβ42 (*m/z*, calcd: 4500.12, found: 4500.32 $[M+H]^+$), K16,K28(*n*L)$_2$-Aβ42 (*m/z*, calcd: 4485.11, found: 4485.13 $[M+H]^+$), R5,K16,K28(*n*L)$_3$-Aβ42 (*m/z*, calcd: 4442.08, found: 4442.58 $[M+H]^+$), ^{13}C,^{15}N labeled-Aβ42 (*m/z*, calcd: 4538.90, found: 4538.94 $[M+H]^+$).

Solid-state NMR Analysis—Aβ42 was labeled at Ala2 ($^{13}C_3$, ^{15}N), Ser8 ($^{13}C_3$, ^{15}N), Lys16 ($^{13}C_6$, $^{15}N_2$), Val18 ($^{13}C_5$, ^{15}N), Phe19, and Phe20 ($^{13}C_{\beta}$).

(+)-Taxifolin was labeled with $^{13}C_6$ on the B-ring as mentioned above (23,24). The labeled Aβ42 (13 μM) was incubated with $^{13}C_6$-(+)-taxifolin (145 μM) in PBS (50 mM sodium phosphate and 100 mM NaCl, pH 7.4) at 37 ^{o}C. After 48 h of incubation, the solution was centrifuged (27,720 *g*, PRP-20-2; Hitachi) for 15 min at 4 ^{o}C, and then the precipitate was dried *in vacuo* to give the labeled Aβ42 aggregate associated with $^{13}C_6$-(+)-taxifolin (12 mg). The solid-state NMR experiments were performed at 14 T (600 MHz for ^{1}H) using a JEOL ECA-600 spectrometer and a custom-fabricated probe with a Chemagnetics 3.2 mm spinning system at a magic angle spinning (MAS) frequency of 21 kHz at room temperature as reported previously (18). The ^{13}C chemical shifts were calibrated in ppm relative to tetramethylsilane by considering the ^{13}C chemical shift for methine ^{13}C of solid adamantine (29.5 ppm) as an external reference. The ^{13}C chemical shifts of labeled Aβ42 and (+)-taxifolin were assigned according to 1D-^{13}C CP/MAS NMR spectra (supplemental Fig. S2A). For the broadband ^{13}C-^{13}C correlation 2D experiments, dipolar-assisted rotational resonance (DARR) was used (36). Pulse sequence parameters of the NMR experiment were as follows; two pulse phase-modulated (TPPM) ^{1}H decoupling power = 80 kHz, RAMP-CP contact time = 1.2 ms, pulse delay = 2 s, t_1 increment = 23.7 μs, t_1 points of 2D = 128 pt, and mixing time (τm) = 50 ms or 500 ms. The window function 'HAMMING' was used in all 2D FT spectra to minimize t_1 noise. As the 2D FT DARR spectra were difficult to analyze because of the t_1 noise (supplemental Fig. S2C), we applied covariance data processing to obtain a better representation of the 2D spectrum (supplemental Fig. S2B). After Fourier transformation along the *t*2 dimension and phase correction, the resulting data matrix was used for covariance processing as previously reported (18,37). The covariance processing step was accelerated by singular value decomposition (38).

Statistical Analyses—All data are presented as the means ± s.e.m. and the differences were analyzed with an one-way analysis of variance (ANOVA) followed by Bonferroni's test or unpaired Student's *t*-test. These tests were implemented within GraphPad Prism software (version 5.0d). *P* values < 0.05 were considered significant.

RESULTS

Effects of Auto-oxidation of (+)-Taxifolin on Its Ability to Prevent the Aggregation of Aβ42—We recently revealed that a catechol moiety on the B-ring of (+)-taxifolin (Fig. 1A) played important role on the inhibitory activity against Aβ42 aggregation (23). A catechol moiety is easily oxidized to form an *o*-quinone (39). To investigate the contribution of auto-oxidation to the inhibitory ability, we examined the aggregative ability of Aβ42 in the presence of (+)-taxifolin treated with sodium periodate ($NaIO_4$), which is known as an oxidant of catechol (40). As shown in Fig. 1B, $NaIO_4$ extensively promoted the suppressive ability of (+)-taxifolin compared with (+)-taxifolin alone. These observations were also confirmed by the TEM experiment (Fig. 2A). $NaIO_4$ treatment in the presence of (+)-taxifolin formed only shorter and thinner fibrils compared with (+)-taxifolin alone. Aβ42 formed the typical fibrils even in the presence of $NaIO_4$ alone, and almost no differences (*e.g.* length, thickness) were observed between the morphology in the presence and absence of $NaIO_4$ (Fig 2A).

$NaIO_4$ alone slightly affected the Th-T fluorescence of Aβ42 aggregates (Fig. 1B) possibly because $NaIO_4$ can oxidize Met35 in Aβ42 to its sulfoxide, the formation of which was confirmed by HPLC (Fig. 1D) and MALDI-TOF-MS (Aβ42-M35^{ox}; *m/z*: calcd: 4531.14, found: 4531.55 $[M+H]^+$). This is in good agreement with a report that oxidation using hydrogen peroxide, a strong oxidant, reduced Aβ42 aggregation (41). However, in the presence of both (+)-taxifolin (50 μM) and $NaIO_4$ (100 μM), Met35 was not oxidized by $NaIO_4$; this was confirmed by HPLC (Fig. 1D) and MALDI-TOF-MS (Aβ42-M35^{red}; *m/z*: calcd: 4515.14, found: 4516.26 $[M+H]^+$). This indicates that $NaIO_4$ preferred to oxidize (+)-taxifolin more than the sulfur atom of the Met35 of Aβ42.

In addition, we tested whether the treatment of $NaIO_4$ leads to the oxidation of Met35 in the preformed Aβ42 fibrils. The fibrils (*ca*. 28 μg) treated with $NaIO_4$ for 4 h were dissolved in formic acid (10 μL), and were sonicated for 1 h. After volatilization, the resultant pellets were resolved in 50% acetonitrile containing 0.1% trifluoroacetic acid, followed by subjection to MALDI-TOF-MS analysis. $NaIO_4$ did not oxidize Met35 in the preformed Aβ42 fibril (Aβ42-M35^{red}; *m/z*: calcd: 4515.14, found: 4515.12 $[M+H]^+$). Also in Th-T assay, Aβ42 fibril was not disassembled by $NaIO_4$ (data not shown). These mean that $NaIO_4$ could partially oxidize Met35 in the monomeric Aβ42, but not the fibrils.

In order to investigate the role of oxygen, suppression of Aβ42 aggregation by (+)-taxifolin was tested *in vacuo*. Notably, (+)-taxifolin little suppressed the aggregation of Aβ42 under an anaerobic condition (Fig. 1C). In TEM images, typical fibril formation was observed even in the presence of (+)-taxifolin under the anaerobic condition (Fig. 2A). Furthermore, Aβ42 aggregated in the presence of (+)-taxifolin and tris(2-carboxyethyl)phosphine (TCEP), a reductant (Fig. 1E). These results suggest the auto-oxidation of (+)-taxifolin to be required for inhibitory activity against Aβ42 aggregation.

The mechanism of Aβ42 fibril formation is well explained by a nucleation-dependent polymerization model mainly consisted of nucleation phase and extension phase (42,43). To determine which stage (nucleation phase or extension phase) was affected by (+)-taxifolin, we examined the effect of (+)-taxifolin on Aβ42 aggregation in the presence of the fibril seed as a template, according to the protocol developed by Naiki *et al*. (30). As shown in Fig 1F, there was a nucleation phase (~1 h) when Aβ42 was incubated alone, whereas addition of the seeds skipped the nucleation phase, resulting in the rapid formation of Aβ42 fibrils. In the case of co-incubation of (+)-taxifolin with the seeds, the nucleation phase of Aβ42 did not drastically change, but the fluorescence gradually decreased after incubation for 4 h, suggesting that (+)-taxifolin could prevent the elongation phase (~2 or 4 h) in Aβ42 aggregation, rather than the nucleation phase (~1 h) (Fig. 1B, F). Although the slight difference of the length of elongation phase between Fig. 1B and 1F might be deduced from several factors, for example, outside temperature, batch (lot) of Aβ42, 2~4 h as an averaged time for elongation phase were observed in another independent experiments. Moreover, we have recently reported the ability of (+)-taxifolin to destabilize the preformed Aβ42 fibril (23). The disappearance of nucleation phase in the presence of seed and $NaIO_4$ (Fig. 1F) implied the ability of oxidized taxilfolin to disassemble even the seed. Indeed, the fluorescence of preformed Aβ42 fibrils immediately disappeared after addition of (+)-taxifolin treated with $NaIO_4$ (data not shown).

Next, we measured UV spectra of (+)-taxifolin incubated with Aβ42 to evaluate the effects of $NaIO_4$ or the anaerobic condition on the auto-oxidation of (+)-taxifolin. When Aβ42 was incubated with (+)-taxifolin under air, the intensity of the peak at 260 nm and 400 nm gradually increased, and that of the peak at 320 nm decreased during 48 h of incubation (Fig. 2B). These spectral changes are characteristic of the oxidation of catechol-type flavonoids to form the *o*-quinone structure (44). The addition of $NaIO_4$ accelerated these UV changes (Fig. 2B). In contrast, there was almost no change in the UV spectra when (+)-taxifolin and Aβ42 were co-incubated *in vacuo* or with TCEP (Fig. 2B). These results indicate that the *o*-quinone formation in (+)-taxifolin through auto-oxidation plays a critical role in the inhibition of Aβ42 aggregation. The UV spectra of Aβ42 alone remained almost constant during the incubation (data not shown), meaning that the spectra of Aβ42 itself did not affect those of (+)-taxifolin.

Conversion to the *o*-quinone from (±)-taxifolin in the presence of $NaIO_4$ was also verified by reacting with *o*-phenylenediamine to yield phenazine (supplemental Scheme S1B), whose structure was confirmed by ^{1}H NMR and HR-EI-MS.

Effects of Auto-oxidation of (+)-Taxifolin on Its Ability to Inhibit Transformation of a Random

Structure into a β-Sheet in Aβ42—We investigated the effects of auto-oxidation of (+)-taxifolin on the secondary structure of Aβ42 by using CD spectroscopy. Shown in Fig. 3A is the data for Aβ42; the positive peak at 195 nm and negative peak at 215 nm drastically increased even after 4 h of incubation, and remained until 48 h of incubation, suggesting that a random structure transformed into a β-sheet in Aβ42. On the other hand, (+)-taxifolin strongly delayed the transformation of Aβ42 (Fig. 3B). Furthermore, addition of $NaIO_4$ decelerated the transformation process during 0~8 h (Fig. 3C).

We also measured the CD spectra under an anaerobic condition (Fig. 3D, E). A spectrum related to the β-sheet formation was found only after 24 h of incubation, but its peak intensity was weaker than that of Aβ42 under air in Fig. 3A. Since radicalization of Aβ42 induced by reactive oxygen species is indispensable to its aggregation (8), these results seem to be reasonable. The transformation into a β-sheet was not suppressed either by (+)-taxifolin *in vacuo*. The findings suggest that the effects of auto-oxidation of (+)-taxifolin on its ability to inhibit Aβ42 aggregation are closely associated with prevention of the transformation into a β-sheet.

LC-MS Analysis of Aβ42 Treated with Oxidized Taxifolin—The *o*-quinone of flavonoids can form covalent bonds with nucleophilic residues in proteins (e.g. Cys, Arg, Lys) to modulate their activity (39,45). Because Aβ42 has three basic amino acid residues (Arg5, Lys16, Lys28), we asked if these residues bound to oxidized taxifolin covalently. The *o*-quinone derived from (+)-taxifolin can react with Lys or Arg residues in Aβ42 through a Michael addition or Schiff base formation (Fig. 4A). We analyzed an Aβ42 solution incubated with (+)-taxifolin and $NaIO_4$ for 4 h using a highly sensitive ion trap type LC-MS equipped with a TOF mass analyzer (LCMS-IT-TOF). As shown in Fig. 4B, LC-MS measurements gave the mass envelop at +7, +6, and +5 charge distribution (deconvoluted mass: 4817.12, calcd: 4816.38), corresponding to the Aβ42–oxidized taxifolin adduct resulted from Michael addition. These results imply that the basic amino acid residues of Aβ42 might be involved in the covalent bonding with the oxidized taxifolin.

Inhibitory Effect of (+)-Taxifolin on Aggregation of Aβ42 Mutants Substituted at Arg5, Lys16, and/or Lys28—Although formation of Michael adducts between the *o*-quinone of (+)-taxifolin and the Lys residues of Aβ42 was suggested in LC-MS (Fig. 4B) together with the verification of the *o*-quinone formation (supplemental Scheme S1B), an attempt to determine the Lys residues involved in the adduct formation by LC-MS-MS analysis was disappointing, possibly because of the extremely low amount and/or instability of the adduct. To obtain further insight into the mechanism by which (+)-taxifolin inhibits the aggregation of Aβ42, we prepared five Aβ42 mutants [R5*n*L-, K16*n*L-, K28*n*L-, K16,K28$(n\mathrm{L})_2$-, and R5,K16,K28$(n\mathrm{L})_3$-Aβ42], where the basic amino acid residues of Aβ42 were substituted with norleucine (*n*L). The aggregative ability in the presence or absence of (+)-taxifolin was also estimated (Figs. 5A-E). These mutants retained substantial aggregative abilities to form fibrils (70~80%) compared with wild-type Aβ42 in Th-T test (Fig. 5F). (+)-Taxifolin did not suppress the aggregative ability of K16*n*L-Aβ42 (Fig. 5B). K28*n*L-Aβ42 also aggregated in the presence of (+)-taxifolin, though intensity of the Th-T fluorescence slightly decreased than that for K28*n*L-Aβ42 alone (Fig. 5C). Moreover, (+)-taxifolin did not prevent the aggregation of K16,K28$(n\mathrm{L})_2$-Aβ42 and R5,K16,K28$(n\mathrm{L})_3$-Aβ42 (Figs. 5D and E). On the other hand, (+)-taxifolin largely suppressed the aggregation of R5*n*L-Aβ42 (Fig. 5A). These results indicate that lysine residues at positions 16 and 28 could be targets for the oxidized taxifolin to prevent the aggregation of Aβ42. More correctly, since the aggregative ability of K28*n*L-Aβ42 was slightly suppressed by (+)-taxifolin compared with that of K16*n*L-Aβ42 (Figs. 5B and C), Lys16 would be more specific target than Lys28 in inhibition of Aβ42 aggregation.

Inhibition of Aβ42 Aggregation by

Non-Catechol-Type Flavonoids—Myricetin, quercetin, morin, and kaempferol, which were previously reported to inhibit Aβ42 aggregation, belong to the flavonols (43). Flavonols contain a double bond between C2 and C3 on the C-ring, whereas flavanonols like (+)-taxifolin do not (Fig. 6A). We calculated IC_{50} for Aβ42 aggregation from the inhibitory rate (%) of each flavonoid [10, 25, 50, 100 μM for a strong-class inhibitor (dihydromyricetin, (+)-taxifolin, myricetin, quercetin); 25, 50, 100, 250 μM for a middle-class inhibitor (morin, kaempferol, datiscetin); 50, 100, 250, 500 μM for a weak-class inhibitor (dihydrokaempferol, pinobanksin, galangin)] on the aggregation of Aβ42 (25 μM) after a 24-h incubation. The values of IC_{50} were summarized in Fig. 6A. Among flavanonols, dihydromyricetin (IC_{50} = 25.3 μM) as well as (+)-taxifolin (IC_{50} = 33.0 μM) with contiguous hydroxyl groups on the B-ring suppressed the aggregation of Aβ42, whereas dihydrokaempferol and pinobanksin (IC_{50} >500 μM) with one or no hydroxyl group did not (Fig. 6A), suggesting vicinal hydroxyl groups on the B-ring to be essential for the inhibitory activity of flavanonols. Similarly, among flavonols, we compared the ability to inhibit Aβ42 aggregation of myricetin, quercetin, morin, kaempferol, datiscetin, and galangin. The aggregation of Aβ42 was strongly suppressed by myricetin (IC_{50} = 15.1 μM) and quercetin (IC_{50} = 15.3 μM) with vicinal hydroxyl groups on the B-ring, while galangin (IC_{50} >500 μM) without a hydroxyl group on the B-ring did not show any inhibitory activity (Fig. 6A). Interestingly, morin (IC_{50} = 30.3 μM), kaempferol (IC_{50} = 75.1 μM), and datiscetin (IC_{50} = 55.4 μM) without a catechol moiety moderately suppressed the aggregation of Aβ42 (Fig. 6A). Regarding the relevance of auto-oxidation to the inhibition of Aβ42 aggregation, we measured the Th-T fluorescence of Aβ42 treated with these three non-catechol-type flavonols under an anaerobic condition or in the presence of TCEP. All these flavonols suppressed the aggregation of Aβ42 even *in vacuo* (Fig. 6B). Moreover, addition of excess of TCEP (Aβ42 : flavonols : TCEP = 25 : 50 : 200 μM) did not affect the suppressive ability of these flavonols (data not shown), indicating that the inhibition of non-catechol-type flavonols could not be ascribed to their auto-oxidation.

To gain further insight into the mechanism by which flavonoids inhibit Aβ42 aggregation by targeting the Lys residues, aggregation tests were carried out in the presence of catechol-type flavonoids (dihydromyricetin, (+)-taxifolin, myricetin or quercetin), or non-catechol-type flavonols (morin, kaempferol, or datiscetin) using K16*n*L- and K16,K28$(n\mathrm{L})_2$-Aβ42. We compared the aggregative ability of Aβ42 mutant (25 μM) incubated with each flavonoid (50 μM), the concentration of which was the maximal value to suppress the fluorescence of Aβ42 under 50% by (+)-taxifolin (data not shown). The catechol-type (+)-taxifolin and quercetin did not suppress the aggregation of these Aβ42 mutants. Although dihydromyricetin and myricetin with contiguous trihydroxyl groups significantly prevented the aggregation of K16*n*L-Aβ42, these flavonoids did not change the aggregative potency of K16,K28$(n\mathrm{L})_2$-Aβ42 (Fig. 7A), implying that they could react with Lys28 as well as Lys16 because contiguous trihydroxyl groups might facilitate the auto-oxidation of the B-ring compared with (+)-taxifolin and quercetin containing vicinal hydroxyl groups. Notably, in the case of non-catechol-type flavonols (morin, kaempferol, and datiscetin), there was little difference in the inhibitory activity among the wild-type, K16*n*L-Aβ42, and K16,K28$(n\mathrm{L})_2$-Aβ42 (Fig. 7B). These results suggest the existence of another inhibitory mechanism for Aβ42 aggregation by non-catechol-type flavonols other than the auto-oxidation followed by the Michael addition of Lys residues, as observed for (+)-taxifolin.

Analysis of the Interaction of Aβ42 Aggregates with (+)-Taxifolin Using Solid-State NMR—Our recent study using a solid-state NMR showed that curcumin with an α,β-unsaturated ketone interacted with the aromatic hydrophobic core (Aβ17-21) due to its inherent hydrophobicity and planarity, resulting in the inhibition of Aβ42 aggregation *via* intercalation (18). Curcumin was reported to interact with Aβ40 fibrils through the planarity of the enol form of curcumin (46).

Also given the preferable detection of monomeric Aβ42 in LC-MS analysis, similar analysis was performed to clarify the interaction between Aβ42 and (+)-taxifolin. (+)-Taxifolin was labeled with $^{13}C_6$ on the B-ring based on the previous structure-activity relationship studies, in which the catechol moiety on the B-ring is critical in the inhibitory potential, and the methylation of hydroxyl group at position 7 on the A-ring did not influence the aggregation of Aβ42 (23). Aβ42 was also ^{13}C-labeled site-specifically at Ala2, Ser8, Lys16, Val18, Phe19, and Phe20, in which only C_β was labeled in Phe19 and Phe20 to avoid the overlapping of the signals of Aβ42 and (+)-taxifolin. For the broadband ^{13}C-^{13}C correlation 2D experiments, dipolar-assisted rotational resonance (DARR) was employed (34). As shown in supplemental Fig. S2B, the interaction peaks between Aβ42 and (+)-taxifolin were as weak as noise signals despite of the use of a ten-fold excess of (+)-taxifolin (Aβ42 : (+)-taxifolin = 13 : 145 μM), while a five-fold excess was employed for curcumin (Aβ42 : curcumin = 10 : 50 μM) (18). Remarkably, the ^{13}C-^{13}C cross peaks between Lys-residues and B-ring of (+)-taxifolin was not observed significantly (Supplemental Fig. S2B). More specifically, the interaction of (+)-taxifolin with the aromatic hydrophobic core (Aβ17-21), which was previously found in the curcumin case due to its inherent hydrophobicity and planarity (18) was not observed. These indicate that the inhibitory mechanism of Aβ42 aggregation by (+)-taxifolin (*via* covalent bonding) could be different from that of curcumin (*via* intercalation).

Since lack of the double bond at positions 2 and 3 of (+)-taxifolin could decreases its planarity, it might not be able to insert into the β-sheet region of the Aβ42 aggregate (Lys16~Ala21). Instability of the oxidized taxifolin–Aβ42 adduct might be another reason. The previous solution-state NMR studies on myricetin and Aβ42 (20) suggested the less-specific broad recognition of the β-sheet region, possibly due to the usage of excessive amounts of myricetin (Aβ42 : myricetin = 25 : 200 μM). This finding might reflect the difference in suppressive ability between myricetin and (+)-taxifolin against K16*n*L-Aβ42 (Fig. 7A).

DISCUSSION

Thus far, the anti-AD activity of flavonoids has been believed to originate from their anti-oxidative activity and/or β-sheet recognition due to their hydrophobicity and planarity. However, these parameters are not necessarily accompanied by the ability to inhibit the aggregation of Aβ42 and other amyloidogenic proteins (11). This background led us to reconsider whether the inhibitory activity can be simply explained by these "less-specific" properties (anti-oxidation, hydrophobicity, and planarity) or not.

On the basis of the present results, we propose a site-specific mechanism whereby catechol-type flavonoids inhibit the aggregation of Aβ42, in which a catechol structure could be auto-oxidized to form the *o*-quinone on the B-ring, followed by the formation of the *o*-quinone-Aβ42 adduct targeting Lys residues at positions 16 and 28 of Aβ42, but not be originated from the anti-oxidative activity (Fig. 8). This could provide unique opportunities to design potent inhibitors of Aβ42 aggregation. On the other hand, the inhibitory ability of non-catechol-type flavonols containing a double bond between C2 and C3 on the C-ring (Fig. 6A) does not require the auto-oxidation. The data in Figs. 6 and 7 indicate that the interaction of non-catechol-type flavonols with Aβ42 might be less effective than the conjugate addition of the Lys residues to the *o*-quinone moiety derived from auto-oxidation. These findings might explain in part the difference in the inhibitory ability between flavanonols and flavonols.

Our previous investigation using solid-state NMR together with systematic proline replacement identified a toxic conformer with a turn at positions 22 and 23 in Aβ42 (47), and proposed that the residues at positions 15-21 and 24-32 containing Lys 16 and Lys 28 are involved in the intermolecular β-sheet region, whereas the N-terminal 13 residues are not (48). A monoclonal antibody against the toxic turn at positions 22 and 23 detected Aβ oligomers in

human AD brain (49) and induced pluripotent stem cells (50) as well as in AD mice (51,52). As mentioned above, an attempt to determine the Lys residues involved in the adduct formation by LC-MS-MS analysis gave disappointing results, possibly because of the extremely low amount and/or instability of the adducts. Since the targeted Lys-residues (Lys16 and 28), not the Arg residue (Arg5), are incorporated in the intermolecular β-sheet region (Fig. 8), even a small amount of covalently-bonded adducts at the Lys residues of Aβ42 oligomers and/or protofibrils could inhibit the formation of Aβ42 aggregates (fibrils) detected by the Th-T fluorescence.

Recently, Bitan's group reported that the Lys-specific synthetic compound (molecular tweezer, CLR01) prevented the cytotoxicity and oligomerization of Aβ42 through non-covalent interaction *in vitro* (53) and *in vivo* (54). Their subsequent study using Aβ42 mutants substituted at Lys16 or Lys28 with Ala revealed a key role for Lys residues in Aβ42-induced neurotoxicity rather than aggregation (55). These reports did not contradict the results that the aggregates of double and triple mutants [K16,K28(nL)$_2$-Aβ42 and R5,K16,K28(nL)$_3$-Aβ42] after 24-h of incubation were slightly less than that of wild-type Aβ42 in this study (Fig. 5F).

R5nL-Aβ42 (~4 h) and K28nL-Aβ42 (~2 h) had the nucleation phase (Fig. 5A, C), while three Aβ42 mutants [K16nL-Aβ42, K16,K28(nL)$_2$-Aβ42, and R5,K16,K28(nL)$_3$-Aβ42] including the substitution of K16 with nL did not (Fig. 5B, D, E). These mean that the aggregative ability of K16nL-Aβ42 seems to be more potent than that of K28nL-Aβ42. Because Lys16 residue is located at a hydrophobic cavity in the β-sheet region (56), the substitution with norleucine without an amino group could enhance the hydrophobic interaction in Aβ42 aggregates, leading to passing the nucleation phase. In contrast, Lys28 was involved in the formation of salt bridge between Asp23 and Lys28 for Aβ42 aggregation (56). These findings imply the different role of lysine resides at positions 16 and 28 in Aβ42 aggregation, which might explain the difference of aggregative ability between K16nL- and K28nL-Aβ42.

Notably, the nucleation phase of R5nL-Aβ42 (~4 h) was partially longer than that of wild-type Aβ42 (~1 h) (Fig. 1B, F and 5A). Since the flexibility of N-terminal region has been thought to be essential for aggregation of Aβ42 (56), the replacement of Arg5 with norleucine might retard the nucleation phase in wild-type Aβ42 aggregation by increasing hydrophobic interaction. Moreover, given no nucleation phase of three Aβ42 mutants of Lys16, it is not surprising that (+)-taxifolin did not largely alter the aggregation properties of these mutants, because (+)-taxifolin could specifically target the elongation phase in wild-type Aβ42 aggregation, rather than the nucleation phase.

LeVine *et al*. suggested preventive effects on Aβ42 aggregation by several dihydroxybenzoic acid isomers, in which 2,3- and 3,4-dihydroxy benzoic acids delayed the velocity of oligomer formation (57). Fisetin, a quercetin analogue without the 5-OH group on the A-ring, also inhibited the aggregation of Aβ42 (58). Ushikubo *et al.* reported that 7-OH group on the A-ring is not involved in the anti-aggregative ability of flavonols (59). These are consistent with our previous study on the structure-activity relationship of (+)-taxifolin (23). On the other hand, lacmoid without a catechol moiety bound less-specifically to Aβ42 (60). These findings together with the present results strongly support that flavonoids with vicinal hydroxyl groups on the B-ring could be indispensable to bind covalently with Aβ42 to suppress its aggregation. It is also reasonable that 3,4,5-trihydroxybenzoic acid, gallic acid (57) and 3',4',5'-trihydroxyflavone (59) as well as dihydromyricetin (Figs. 6A) suppressed the aggregation of wild-type Aβ42. In particular, the inhibitory activities of dihydromyricetin, (+)-taxifolin, myricetin, and quercetin were higher than those of morin, kampferol, and datiscetin (Fig. 6A), suggesting that the nucleophilic addition to the *o*-quinone moiety by the Lys residues of Aβ42 could contribute more significantly to the inhibition of Aβ42 aggregation than the hydrophobic interaction.

However, additional role of the A- and C-rings of catechol-type flavonoids in the suppression of Aβ42 aggregation is not negligible, since the inhibitory activity of catechol itself was low (61).

Fink and colleagues previously proposed the contribution of interaction of Lys residues with the baicalein *o*-quinone to the inhibition of α-synuclein responsible for Parkinson's disease (45). However, the underlying molecular mechanism cannot be fully explained by the oxidized baicalein because the aggregation of α-synuclein was inhibited by baicalein even under an anaerobic condition (45). Quite recently, the oxidation product of EGCG was in part involved in remodeling the preformed fibrils of Aβ40 by EGCG (62).

To the best of our knowledge, this is a first report that dihydromyricetin and datiscetin as well as (+)-taxifolin have anti-aggregative activity against Aβ42. We also demonstrated that (+)-taxifolin could suppress the elongation phase in the aggregation of wild-type Aβ42, rather than the nucleation phase. Seed extracts of *Silybum marianum*, known as silymarin, have long been used as an anti-hepatotoxic medicine without notable adverse effects (63), and in particular, are efficacious against damage induced by alcohol and disturbances in the function of the gastrointestinal tract (64). Booth *et al*. showed that (+)-taxifolin was not toxic when given long term to albino rats (65). Therefore, (+)-taxifolin may be a worthy candidate for AD therapeutics. Although some polyphenols [naringenin (66) and curcumin (67)] were reported to pass through the blood-brain barrier after oral administration, caution should be used because of the difference between animal and clinical condition.

REFERENCES

1. Glenner, G. G., and Wong, C. W. (1984) Alzheimer's disease: initial report of the purification and characterization of a novel cerebrovascular amyloid protein. *Biochem. Biophys. Res. Commun.* **120**, 885-890
2. Masters, C. L., Simms, G., Weinman, N. A., Multhaup, G., McDonald, B. L., and Beyreuther, K. (1985) Amyloid plaque core protein in Alzheimer disease and Down syndrome. *Proc. Natl. Acad. Sci. USA* **82**, 4245-4249
3. Haass, C., and Selkoe, D. J. (2007) Soluble protein oligomers in neurodegeneration: lessons from the Alzheimer's amyloid β-peptide. *Nat. Rev. Mol. Cell Biol.* **8**, 101-112
4. Walsh, D. M., Klyubin, I., Fadeeva, J. V., Cullen, W. K., Anwyl, R., Wolfe, M. S., Rowan, M. J., and Selkoe, D. J. (2002) Naturally secreted oligomers of amyloid β protein potently inhibit hippocampal long-term potentiation *in vivo*. *Nature* **416**, 535-539
5. Roychaudhuri, R., Yang, M., Hoshi, M. M., and Teplow, D. B. (2009) Amyloid β-protein assembly and Alzheimer disease. *J. Biol. Chem.* **284**, 4749-4753
6. Sayre, L. M., Perry, G., and Smith, M. A. (2007) Oxidative stress and neurotoxicity. *Chem. Res. Toxicol.* **21**, 172-188
7. Varadarajan, S., Yatin, S., Aksenova, M., and Butterfield, D. A. (2000) Review: Alzheimer's amyloid β-peptide-associated free radical oxidative stress and neurotoxicity. *J. Struct. Biol.* **130**, 184-208
8. Murakami, K., Irie, K., Ohigashi, H., Hara, H., Nagao, M., Shimizu, T., and Shirasawa, T. (2005) Formation and stabilization model of the 42-mer Aβ radical: Implications for the long-lasting oxidative stress in Alzheimer's disease. *J. Am. Chem. Soc.* **127**, 15168-15174
9. Li, F., Calingasan, N. Y., Yu, F., Mauck, W. M., Toidze, M., Almeida, C. G., Takahashi, R. H., Carlson, G. A., Flint Beal, M., Lin, M. T., and Gouras, G. K. (2004) Increased plaque burden in brains of APP mutant MnSOD heterozygous knockout mice. *J. Neurochem.* **89**, 1308-1312
10. Murakami, K., Murata, N., Noda, Y., Tahara, S., Kaneko, T., Kinoshita, N., Hatsuta, H.,

Murayama, S., Barnham, K. J., Irie, K., Shirasawa, T., and Shimizu, T. (2011) SOD1 (Copper/zinc superoxide dismutase) deficiency drives amyloid β protein oligomerizfation and memory loss in mouse model of Alzheimer disease. *J. Biol. Chem.* **286**, 44557-44568

11. Porat, Y., Abramowitz, A., and Gazit, E. (2006) Inhibition of amyloid fibril formation by polyphenols: structural similarity and aromatic interactions as a common inhibition mechanism. *Chem. Biol. Drug Des.* **67**, 27-37
12. Rossi, L., Mazzitelli, S., Arciello, M., Capo, C. R., and Rotilio, G. (2008) Benefits from dietary polyphenols for brain aging and Alzheimer's disease. *Neurochem. Res.* **33**, 2390-2400
13. Williams, R. J., and Spencer, J. P. E. (2012) Flavonoids, cognition, and dementia: actions, mechanisms, and potential therapeutic utility for Alzheimer disease. *Free Radic. Biol. Med.* **52**, 35-45
14. Gravitz, L. (2011) Drugs: A tangled web of targets. *Nature* **475**, S9-S11
15. Mecocci, P., and Polidori, M. C. (2012) Antioxidant clinical trials in mild cognitive impairment and Alzheimer's disease. *Biochim. Biophys. Acta* **1822**, 631-638
16. Grill, J. D., and Cummings, J. L. (2010) Current therapeutic targets for the treatment of Alzheimer's disease. *Expert Rev. Neurother.* **10**, 711-728
17. Keshet, B., Gray, J. J., and Good, T. A. (2010) Structurally distinct toxicity inhibitors bind at common loci on β-amyloid fibril. *Protein Sci.* **19**, 2291-2304
18. Masuda, Y., Fukuchi, M., Yatagawa, T., Tada, M., Takeda, K., Irie, K., Akagi, K., Monobe, Y., Imazawa, T., and Takegoshi, K. (2011) Solid-state NMR analysis of interaction sites of curcumin and 42-residue amyloid β-protein fibrils. *Biorg. Med. Chem.* **19**, 5967-5974
19. Lopez del Amo, J. M., Fink, U., Dasari, M., Grelle, G., Wanker, E. E., Bieschke, J., and Reif, B. (2012) Structural properties of EGCG-induced, nontoxic Alzheimer's disease Aβ oligomers. *J. Mol. Biol.* **421**, 517-524
20. Ono, K., Li, L., Takamura, Y., Yoshiike, Y., Zhu, L., Han, F., Mao, X., Ikeda, T., Takasaki, J., Nishijo, H., Takashima, A., Teplow, D. B., Zagorski, M. G., and Yamada, M. (2012) Phenolic compounds prevent amyloid β-protein oligomerization and synaptic dysfunction by site-specific binding. *J. Biol. Chem.* **287**, 14631-14643
21. Murata, N., Murakami, K., Ozawa, Y., Kinoshita, N., Irie, K., Shirasawa, T., and Shimizu, T. (2010) Silymarin attenuated the amyloid β plaque burden and improved behavioral abnormalities in an Alzheimer's disease mouse model. *Biosci. Biotechnol. Biochem.* **74**, 2299-2306
22. Kim, N.-C., Graf, T. N., Sparacino, C. M., Wani, M. C., and Wall, M. E. (2003) Complete isolation and characterization of silybins and isosilybins from milk thistle (*Silybum marianum*). *Org. Biomol. Chem.* **1**, 1684-1689
23. Sato, M., Murakami, K., Uno, M., Ikubo, H., Nakagawa, Y., Katayama, S., Akagi, K., and Irie, K. (2013) Structure-Activity Relationship for (+)-Taxifolin Isolated from Silymarin as an Inhibitor of Amyloid β Aggregation. *Biosci. Biotechnol. Biochem.* **77**, 1100-1103
24. Roschek Jr, B., Fink, R. C., McMichael, M. D., Li, D., and Alberte, R. S. (2009) Elderberry flavonoids bind to and prevent H1N1 infection *in vitro*. *Phytochemistry* **70**, 1255-1261
25. Vega-Villa, K. R., Remsberg, C. M., Ohgami, Y., Yanez, J. A., Takemoto, J. K., Andrews, P. K., and Davies, N. M. (2009) Stereospecific high-performance liquid chromatography of taxifolin, applications in pharmacokinetics, and determination in tu fu ling (*Rhizoma smilacis glabrae*) and apple (*Malus x domestica*). *Biomed. Chromatogr.* **23**, 638-646
26. Jeon, S., Chun, W., Choi, Y., and Kwon, Y. (2008) Cytotoxic constituents from the bark of *Salix hulteni*. *Arch. Pharm. Res.* **31**, 978-982
27. Kuroyanagi, M., Yamamoto, Y., Fukushima, S., Ueno, A., Noro, T., and Miyase, T. (1982) Chemical Studies on the Constituents of Polygonum nodosum. *Chem. Pharm. Bull.* **30**, 1602-1608

28. Kiehlmann, E., and Slade, P. W. (2003) Methylation of dihydroquercetin acetates: Synthesis of 5-*O*-methyldihydroquercetin. *J. Nat. Prod.* **66**, 1562-1566
29. Markham, K. R., and Ternai, B. (1976) ^{13}C NMR of flavonoids—II : Flavonoids other then flavone and flavonol aglycones. *Tetrahedron* **32**, 2607-2612
30. Naiki, H., and Gejyo, F. (1999) [20] Kinetic analysis of amyloid fibril formation. *Methods Enzymol.* 305-318
31. Murakami, K., Irie, K., Morimoto, A., Ohigashi, H., Shindo, M., Nagao, M., Shimizu, T., and Shirasawa, T. (2003) Neurotoxicity and physicochemical properties of Aβ mutant peptides from cerebral amyloid angiopathy. *J. Biol. Chem.* **278**, 46179-46187
32. Murakami, K., Irie, K., Morimoto, A., Ohigashi, H., Shindo, M., Nagao, M., Shimizu, T., and Shirasawa, T. (2002) Synthesis, aggregation, neurotoxicity, and secondary structure of various Aβ1–42 mutants of familial Alzheimer's disease at positions 21–23. *Biochem. Biophys. Res. Commun.* **294**, 5-10
33. Fields, C. G., Fields, G. B., Noble, R. L., and Cross, T. A. (1989) Solid phase peptide synthesis of ^{15}N-gramicidins A, B, and C and high performance liquid chromatographic purification. *Int. J. Pept. Protein Res.* **33**, 298-303
34. Wiejak, S., Masiukiewicz, E., and Rzeszotarska, B. (1999) A large scale synthesis of mono- and di-urethane derivatives of lysine. *Chem. Pharm. Bull.* **47**, 1489-1490
35. Irie, K., Oie, K., Nakahara, A., Yanai, Y., Ohigashi, H., Wender, P. A., Fukuda, H., Konishi, H., and Kikkawa, U. (1998) Molecular basis for protein kinase C isozyme-selective binding: the synthesis, folding, and phorbol ester binding of the cysteine-rich domeins of all protein kinase C isozymes. *J. Am. Chem. Soc.* **120**, 9159-9167
36. Takegoshi, K., Nakamura, S., and Terao, T. (2001) ^{13}C–^{1}H dipolar-assisted rotational resonance in magic-angle spinning NMR. *Chem. Phys. Lett.* **344**, 631-637
37. Bruschweiler, R. (2004) Theory of covariance nuclear magnetic resonance spectroscopy. *J. Chem. Phys.* **121**, 409-414
38. Trbovic, N., Smirnov, S., Zhang, F., and Brüschweiler, R. (2004) Covariance NMR spectroscopy by singular value decomposition. *J. Magn. Res.* **171**, 277-283
39. Ishii, T., Mori, T., Tanaka, T., Mizuno, D., Yamaji, R., Kumazawa, S., Nakayama, T., and Akagawa, M. (2008) Covalent modification of proteins by green tea polyphenol (-)-epigallocatechin-3-gallate through autoxidation. *Free Radic. Biol. Med.* **45**, 1384-1394
40. Graham, D. G., and Jeffs, P. W. (1977) The role of 2,4,5-trihydroxyphenylalanine in melanin biosynthesis. *J. Biol. Chem.* **252**, 5729-5734
41. Hou, L., Kang, I., Marchant, R. E., and Zagorski, M. G. (2002) Methionine 35 oxidation reduces fibril assembly of the amyloid Aβ-(1–42) peptide of Alzheimer's disease. *J. Biol. Chem.* **277**, 40173-40176
42. Hasegawa, K., Yamaguchi, I., Omata, S., Gejyo, F., and Naiki, H. (1999) Interaction between Aβ(1−42) and Aβ(1−40) in Alzheimer's β-Amyloid Fibril Formation in Vitro. *Biochemistry* **38**, 15514-15521
43. Ono, K., Hamaguchi, T., Naiki, H., and Yamada, M. (2006) Anti-amyloidogenic effects of antioxidants: implications for the prevention and therapeutics of Alzheimer's disease. *Biochim. Biophys. Acta* **1762**, 575-586
44. Kostyuk, V. A., Kraemer, T., Sies, H., and Schewe, T. (2003) Myeloperoxidase/nitrite-mediated lipid peroxidation of low-density lipoprotein as modulated by flavonoids. *FEBS Lett.* **537**, 146-150
45. Zhu, M., Rajamani, S., Kaylor, J., Han, S., Zhou, F., and Fink, A. L. (2004) The flavonoid baicalein inhibits fibrillation of α-synuclein and disaggregates existing fibrils. *J. Biol. Chem.* **279**, 26846-26857

46. Yanagisawa, D., Shirai, N., Amatsubo, T., Taguchi, H., Hirao, K., Urushitani, M., Morikawa, S., Inubushi, T., Kato, M., Kato, F., Morino, K., Kimura, H., Nakano, I., Yoshida, C., Okada, T., Sano, M., Wada, Y., Wada, K., Yamamoto, A., and Tooyama, I. (2010) Relationship between the tautomeric structures of curcumin derivatives and their Aβ-binding activities in the context of therapies for Alzheimer's disease. *Biomaterials* **31**, 4179-4185
47. Masuda, Y., Uemura, S., Ohashi, R., Nakanishi, A., Takegoshi, K., Shimizu, T., Shirasawa, T., and Irie, K. (2009) Identification of physiological and toxic conformations in Aβ42 aggregates. *ChemBioChem* **10**, 287-295
48. Morimoto, A., Irie, K., Murakami, K., Masuda, Y., Ohigashi, H., Nagao, M., Fukuda, H., Shimizu, T., and Shirasawa, T. (2004) Analysis of the secondary structure of β-amyloid (Aβ42) fibrils by systematic proline replacement. *J. Biol. Chem.* **279**, 52781-52788
49. Murakami, K., Horikoshi-Sakuraba, Y., Murata, N., Noda, Y., Masuda, Y., Kinoshita, N., Hatsuta, H., Murayama, S., Shirasawa, T., Shimizu, T., and Irie, K. (2010) Monoclonal antibody against the turn of the 42-residue amyloid β-Ppotein at positions 22 and 23. *ACS Chem. Neurosci.* **1**, 747-756
50. Kondo, T., Asai, M., Tsukita, K., Kutoku, Y., Ohsawa, Y., Sunada, Y., Imamura, K., Egawa, N., Yahata, N., Okita, K., Takahashi, K., Asaka, I., Aoi, T., Watanabe, A., Watanabe, K., Kadoya, C., Nakano, R., Watanabe, D., Maruyama, K., Hori, O., Hibino, S., Choshi, T., Nakahata, T., Hioki, H., Kaneko, T., Naitoh, M., Yoshikawa, K., Yamawaki, S., Suzuki, S., Hata, R., Ueno, S., Seki, T., Kobayashi, K., Toda, T., Murakami, K., Irie, K., Klein, William L., Mori, H., Asada, T., Takahashi, R., Iwata, N., Yamanaka, S., and Inoue, H. (2013) Modeling Alzheimer s Disease with iPSCs Reveals Stress Phenotypes Associated with Intracellular Aβ and Differential Drug Responsiveness. *Cell stem cell* **12**, 487-492
51. Kulic, L., McAfoose, J., Welt, T., Tackenberg, C., Spani, C., Wirth, F., Finder, V., Konietzko, U., Giese, M., Eckert, A., Noriaki, K., Shimizu, T., Murakami, K., Irie, K., Rasool, S., Glabe, C., Hock, C., and Nitsch, R. M. (2012) Early accumulation of intracellular fibrillar oligomers and late congophilic amyloid angiopathy in mice expressing the Osaka intra-Aβ APP mutation. *Transl. Psychiatry* **2**, e183
52. Soejima, N., Ohyagi, Y., Nakamura, N., Himeno, E., M. Iinuma, K., Sakae, N., Yamasaki, R., Tabira, T., Murakami, K., Irie, K., Kinoshita, N., M. LaFerla, F., Kiyohara, Y., Iwaki, T., and Kira, J. (2013) Intracellular Accumulation of Toxic Turn Amyloid-β is Associated with Endoplasmic Reticulum Stress in Alzheimers Disease. *Curr. Alzheimer Res.* **10**, 11-20
53. Sinha, S., Lopes, D. H., Du, Z., Pang, E. S., Shanmugam, A., Lomakin, A., Talbiersky, P., Tennstaedt, A., McDaniel, K., Bakshi, R., Kuo, P. Y., Ehrmann, M., Benedek, G. B., Loo, J. A., Klarner, F. G., Schrader, T., Wang, C., and Bitan, G. (2011) Lysine-specific molecular tweezers are broad-spectrum inhibitors of assembly and toxicity of amyloid proteins. *J. Am. Chem. Soc.* **133**, 16958-16969
54. Attar, A., Ripoli, C., Riccardi, E., Maiti, P., Li Puma, D. D., Liu, T., Hayes, J., Jones, M. R., Lichti-Kaiser, K., Yang, F., Gale, G. D., Tseng, C. H., Tan, M., Xie, C. W., Straudinger, J. L., Klarner, F. G., Schrader, T., Frautschy, S. A., Grassi, C., and Bitan, G. (2012) Protection of primary neurons and mouse brain from Alzheimer's pathology by molecular tweezers. *Brain* **135**, 3735-3748
55. Sinha, S., Lopes, D. H. J., and Bitan, G. (2012) A key role for lysine residues in amyloid β-protein folding, assembly, and toxicity. *ACS Chem. Neurosci.* **3**, 473-481
56. Petkova, A. T., Ishii, Y., Balbach, J. J., Antzutkin, O. N., Leapman, R. D., Delaglio, F., and Tycko, R. (2002) A structural model for Alzheimer's β-amyloid fibrils based on experimental constraints from solid state NMR. *Proc. Natl. Acad. Sci. USA* **99**, 16742-16747
57. LeVine, H., Lampe, L., Abdelmoti, L., and Augelli-Szafran, C. E. (2012) Dihydroxybenzoic acid

isomers differentially dissociate soluble biotinyl-Aβ(1–42) oligomers. *Biochemistry* **51**, 307-315
58. Akaishi, T., Morimoto, T., Shibao, M., Watanabe, S., Sakai-Kato, K., Utsunomiya-Tate, N., and Abe, K. (2008) Structural requirements for the flavonoid fisetin in inhibiting fibril formation of amyloid β protein. *Neurosci. Lett.* **444**, 280-285
59. Ushikubo, H., Watanabe, S., Tanimoto, Y., Abe, K., Hiza, A., Ogawa, T., Asakawa, T., Kan, T., and Akaishi, T. (2012) 3,3',4',5,5'-Pentahydroxyflavone is a potent inhibitor of amyloid β fibril formation. *Neurosci. Lett.* **513**, 51-56
60. Abelein, A., Bolognesi, B., Dobson, C. M., Gräslund, A., and Lendel, C. (2012) Hydrophobicity and conformational change as mechanistic determinants for nonspecific modulators of amyloid β self-assembly. *Biochemistry* **51**, 126-137
61. Huong, V. T., Shimanouchi, T., Shimauchi, N., Yagi, H., Umakoshi, H., Goto, Y., and Kuboi, R. (2010) Catechol derivatives inhibit the fibril formation of amyloid-β peptides. *J. Biosci. Bioeng.* **109**, 629-634
62. Palhano, F. L., Lee, J., Grimster, N. P., and Kelly, J. W. (2013) Toward the Molecular Mechanism(s) by Which EGCG Treatment Remodels Mature Amyloid Fibrils. *J. Am. Chem. Soc.* **135**, 7503-7510
63. Morazzoni, P., Montalbetti, A., Malandrino, S., and Pifferi, G. (1993) Comparative pharmacokinetics of silipide and silymarin in rats. *Eur. J. Drug Metabol. Pharmacokinet.* **18**, 289-297
64. Valenzuela, A., Barría, T., Guerra, R., and Garrido, A. (1985) Inhibitory effect of the flavonoid silymarin on the erythrocyte hemolysis induced by phenylhydrazine. *Biochem. Biophys. Res. Commun.* **126**, 712-718
65. Booth, A. N., and Deeds, F. (1958) The toxicity and metabolism of dihydroquercetin. *J. Am. Pharm. Assoc.* **47**, 183-184
66. Youdim, K. A., Shukitt-Hale, B., and Joseph, J. A. (2004) Flavonoids and the brain: interactions at the blood-brain barrier and their physiological effects on the central nervous system. *Free Radic. Biol. Med.* **37**, 1683-1693
67. Yang, F., Lim, G. P., Begum, A. N., Ubeda, O. J., Simmons, M. R., Ambegaokar, S. S., Chen, P. P., Kayed, R., Glabe, C. G., Frautschy, S. A., and Cole, G. M. (2005) Curcumin inhibits formation of amyloid β oligomers and fibrils, binds plaques, and reduces amyloid *in vivo*. *J. Biol. Chem.* **280**, 5892-5901

FOOTNOTES

*We thank Prof. Nobutaka Fujii and Dr. Shinya Oishi from Graduate School of Pharmaceutical Sciences, Kyoto University for use of MALDI-TOF-MS and LC-MS. This study was supported in part by Grants-in-Aid for Scientific Research (A) (Grant No. 21248015 to K. I.), and (C) (No. 22603006 to K. M.), and a fund for the Promotion of Science for Young Scientists (Grant No. 22.4068 to M. S.) from The Ministry of Education, Culture, Sports, Science and Technology, Japan, and by funds from Asahi Beer Science Promotion Foundation (to K. I.) and from Kato Memorial Bioscience Foundation (to K. M.).

[†]Research Fellow of the Japan Society for the Promotion of Science.

[1]The abbreviations used are: Aβ, amyloid β-protein; AD, Alzheimer's disease; ANOVA, analysis of variance; CD, circular dichroism; EGCG, (-)-epigallocatechin-3-gallate; EI-MS, electron ionization-mass spectrometry; HPLC, high performance liquid chromatography; LC-MS, liquid chromatography-mass spectrometry; MALDI-TOF-MS, matrix-assisted laser desorption/ionization time-of-flight mass spectrometry; NMR, nuclear magnetic resonance; PBS, phosphate-buffered saline; TCEP, tris(2-carboxyethyl)phosphate; TEM, transmission electron microscopy; Th-T, thioflavin-T; UV, ultraviolet.

FIGURE LEGENDS

Fig. 1. Effects of auto-oxidation of (+)-taxifolin on its ability to inhibit Aβ42 aggregation and Met35 oxidation. ***A,*** The structure of (+)-taxifolin. ***B,*** The effect of sodium periodate ($NaIO_4$), an oxidant, on Aβ42 aggregation estimated by Th-T tests. Aβ42 (25 μM) was incubated with or without (+)-taxifolin (50 μM) and/or $NaIO_4$ (100 μM) at 37 °C. ***C,*** The ability of (+)-taxifolin to suppress the aggregation of Aβ42 under an anaerobic condition. Aβ42 (25 μM) was incubated with or without (+)-taxifolin (50 μM) *in vacuo* at room temperature. ***D,*** HPLC analysis of Aβ42 solution with the indicated treatment. Aβ42 (25 μM) was incubated with or without (+)-taxifolin (50 μM) and/or $NaIO_4$ (100 μM) at 37 °C for 4 h. An aliquot was centrifuged by 20,130 *g* at 4 °C for 10 min, and the supernatant was subjected to HPLC on a Develosil ODS UG-5 column under a gradient of 10-50% CH_3CN containing 0.1% NH_4OH for 40 min. ***E,*** The effect of tris(2-carboxylethyl)phosphine hydrochloride (TCEP-HCl denoted as TCEP), a reductant, on Aβ42 aggregation. Aβ42 (25 μM) was incubated with or without (+)-taxioflin (50 μM) and/or TCEP (100 μM) at 37 °C. ***F,*** The aggregative ability of Aβ42 in the presence of Aβ42 seed and/or (+)-taxifolin, $NaIO_4$. Aβ42 (25 μM) was incubated with or without the seed (10 μg/mL) and/or (+)-taxifolin (50 μM), $NaIO_4$ (100 μM) at 37 °C. The data are presented as the mean ± s.e.m. (n = 8). Th-T relative fluorescence was expressed as a percentage of the fluorescence for wild-type Aβ42 alone, whose maximum value was taken as 100%.

Fig. 2. Effects of auto-oxidation of (+)-taxifolin on the morphology of Aβ42 aggregates. ***A,*** TEM images of Aβ42 aggregates after 48 h of incubation. Aβ42 (25 μM) was treated with or without (+)-taxifolin (50 μM) and/or $NaIO_4$ (100 μM) under an aerobic or anaerobic condition. Scale bar = 200 nm. ***B,*** UV-visible spectra of (+)-taxifolin (50 μM) treated with Aβ42 (25 μM) in the presence of $NaIO_4$ (100 μM) or TCEP (100 μM) after incubation for 0, 4, 8, 24, and 48 h, respectively.

Fig. 3. Effects of auto-oxidation of (+)-taxifolin on its ability to prevent the transformation into the β-sheet structure of Aβ42 using CD spectrometry. ***A-C,*** Aβ42 (25 μM) was incubated (***A***) without, with (+)-taxifolin (50 μM) in the (***B***) absence or (***C***) presence of $NaIO_4$ (100 μM) at 37 °C for the period indicated. ***D, E,*** Aβ42 (25 μM) was incubated (***D***) without or (***E***) with (+)-taxifolin (50 μM) *in vacuo* at room temperature for the period indicated.

Fig. 4. LC-MS analysis of Aβ42 treated with oxidized taxifolin. ***A,*** The proposed structures of the adducts between oxidized taxifolin and Aβ42. (*Upper*) Lys16, Lys28, and (*lower*) Arg5 in Aβ42 could attack the *o*-quinone of (+)-taxifolin, resulting in (*left*) Michael addition or (*right*) Schiff base formation with the indicated calculated mass. ***B,*** LCMS-IT-TOF analysis of the Aβ42 solution treated with oxidized taxifolin. After Aβ42 (25 μM) was incubated with (+)-taxifolin (50 μM) in the presence of $NaIO_4$ (100 μM) at 37 °C for 4 h, an aliquot was subjected to the analysis.

Fig. 5. Effects of (+)-taxifolin on the aggregation of Aβ42 mutants substituted with norleucine (*n*L). The aggregative ability of ***A,*** R5*n*L-Aβ42, ***B,*** K16*n*L-Aβ42, ***C,*** K28*n*L-Aβ42, ***D,*** K16,K28(nL)$_2$-Aβ42, and ***E,*** R5,K16,K28(nL)$_3$-Aβ42 in the presence of (+)-taxifolin was examined by Th-T assay. Each Aβ42 mutant (25 μM) was incubated with or without (+)-taxifolin (50 μM) at 37 °C. The data are presented as the mean ± s.e.m. (n = 8). Th-T relative fluorescence was expressed as a percentage of the fluorescence for Aβ42 mutant alone, whose maximum value was taken as 100%. *p<0.05 compared with Aβ42 mutant alone. The time point without asterisk means no significant difference between Aβ42 mutant treated and untreated with (+)-taxifolin. ***F,*** The comparison of

aggregative ability of Aβ42 mutants. Th-T relative fluorescence of each mutant after incubation for 24 h was expressed as a percentage of the fluorescence for wild-type Aβ42 alone, whose maximum value was taken as 100%. The data are presented as the mean ± s.e.m. (n = 8).

Fig. 6. Effects of flavanonols and flavonols on the aggregation of Aβ42. ***A,*** The structures and IC_{50} values of (*upper*) flavanonols and (*lower*) flavonols examined in this study. The IC_{50} value was calculated from the inhibitory rate (%) of each flavonoid on Aβ42 aggregation after 24 h incubation using Th-T assay. ***B,*** Aβ42 (25 μM) incubated with morin, kaempferol, or datiscetin (50 μM) *in vacuo* at room temperature. Th-T relative fluorescence was expressed as a percentage of the fluorescence for Aβ42 alone, whose maximum value was taken as 100%.

Fig. 7. Effects of flavanonols and flavonols on the aggregation of Aβ42 mutants. ***A,*** The aggregative ability of Aβ42 mutants (25 μM) incubated with a catechol-type flavanonol or flavonol (50 μM) for 24 h estimated by Th-T tests. The data are presented as the mean ± s.e.m. (n = 8). Th-T relative fluorescence was expressed as a percentage of the fluorescence for each Aβ42 alone, whose value at 24 h was taken as 100%. ***B,*** The aggregative ability of Aβ42 mutants (25 μM) treated with a non-catechol-type flavonol (50 μM) for 24 h, estimated by Th-T tests. *p<0.05. n.s. = not significant.

Fig. 8. Site-specific inhibitory mechanisms of Aβ42 aggregation by catechol-type flavonoids. Catechol-type flavanonols (*e.g.* (+)-taxifolin) or flavonols (*e.g.* quercetin) were oxidized to form corresponding *o*-quinones on B-ring, followed by the formation of adducts by Lys16 and Lys28 of Aβ42. Because Lys16 and Lys28 are incorporated in the intermolecular β-sheet region (8), Aβ42 aggregates would be destabilized by the adduct formation.

Figure 1

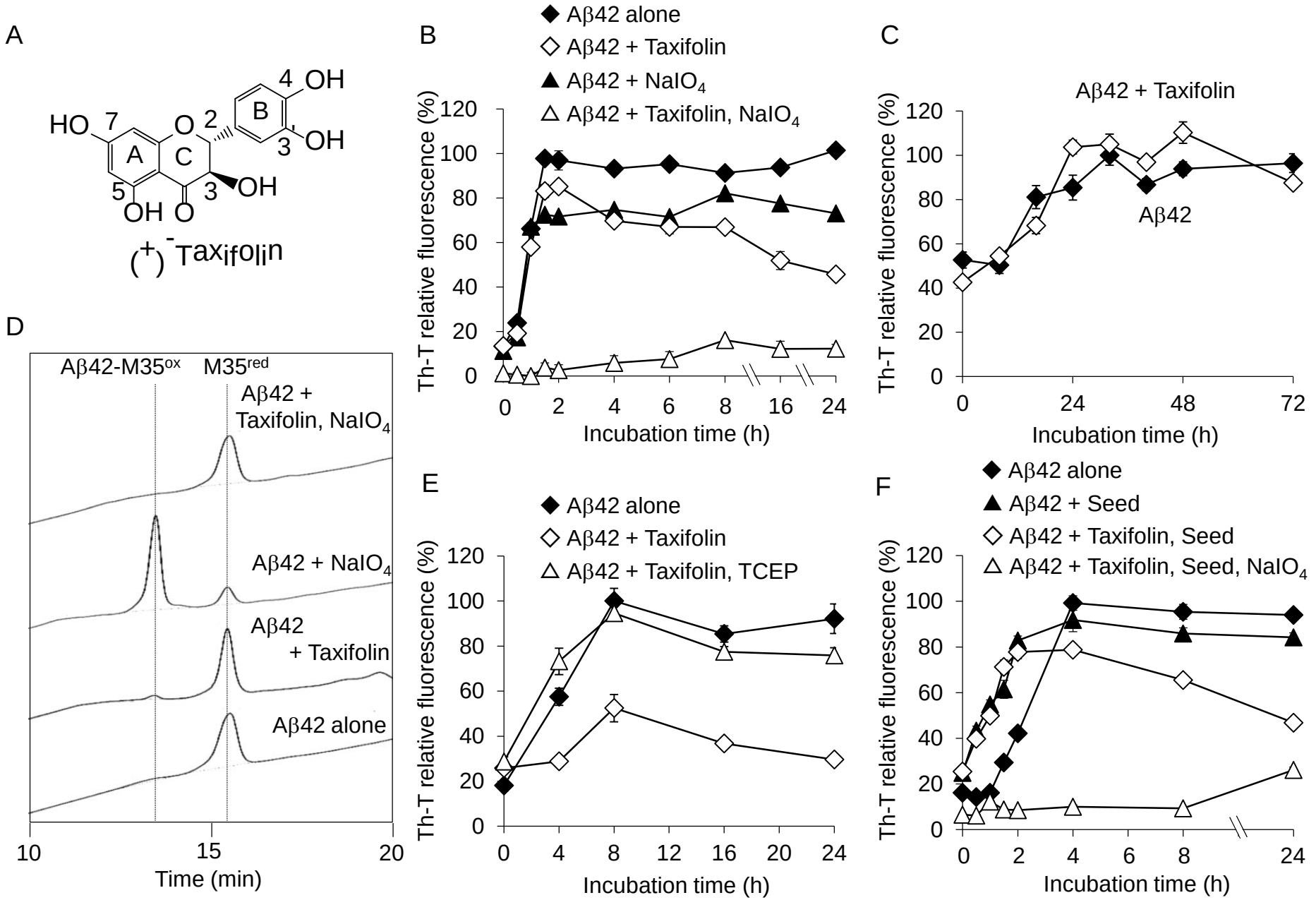
A
HO
7
O
2
B
4 OH
3 OH
A
C
5
OH
3
OH
O
(+)-Taxifolin
B
Aβ42 alone
Aβ42 + Taxifolin
Aβ42 + NaIO4
Aβ42 + Taxifolin, NaIO4
Th-T relative fluorescence (%)
Incubation time (h)
C
Aβ42 + Taxifolin
Aβ42
Th-T relative fluorescence (%)
Incubation time (h)
D
Aβ42-M35ox
M35red
Aβ42 + Taxifolin, NaIO4
Aβ42 + NaIO4
Aβ42 + Taxifolin
Aβ42 alone
Time (min)
E
Aβ42 alone
Aβ42 + Taxifolin
Aβ42 + Taxifolin, TCEP
Th-T relative fluorescence (%)
Incubation time (h)
F
Aβ42 alone
Aβ42 + Seed
Aβ42 + Taxifolin, Seed
Aβ42 + Taxifolin, Seed, NaIO4
Th-T relative fluorescence (%)
Incubation time (h)

Figure 2

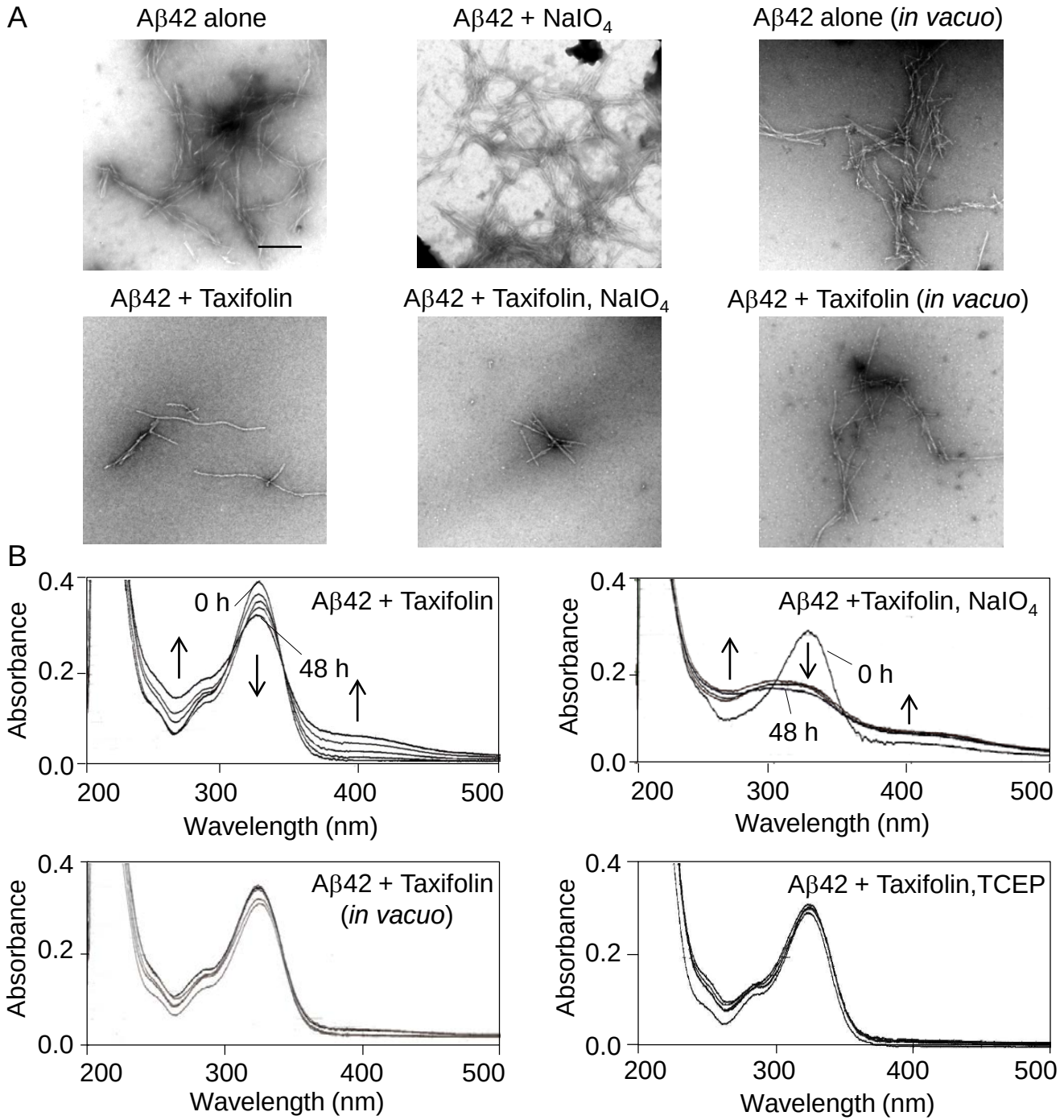
A
Aβ42 alone
Aβ42 + NaIO4
Aβ42 alone (in vacuo)
Aβ42 + Taxifolin
Aβ42 + Taxifolin, NaIO4
Aβ42 + Taxifolin (in vacuo)
B
Absorbance
Wavelength (nm)
0 h
48 h
Aβ42 + Taxifolin
Aβ42 +Taxifolin, NaIO4
Aβ42 + Taxifolin (in vacuo)
Aβ42 + Taxifolin,TCEP

Figure 3

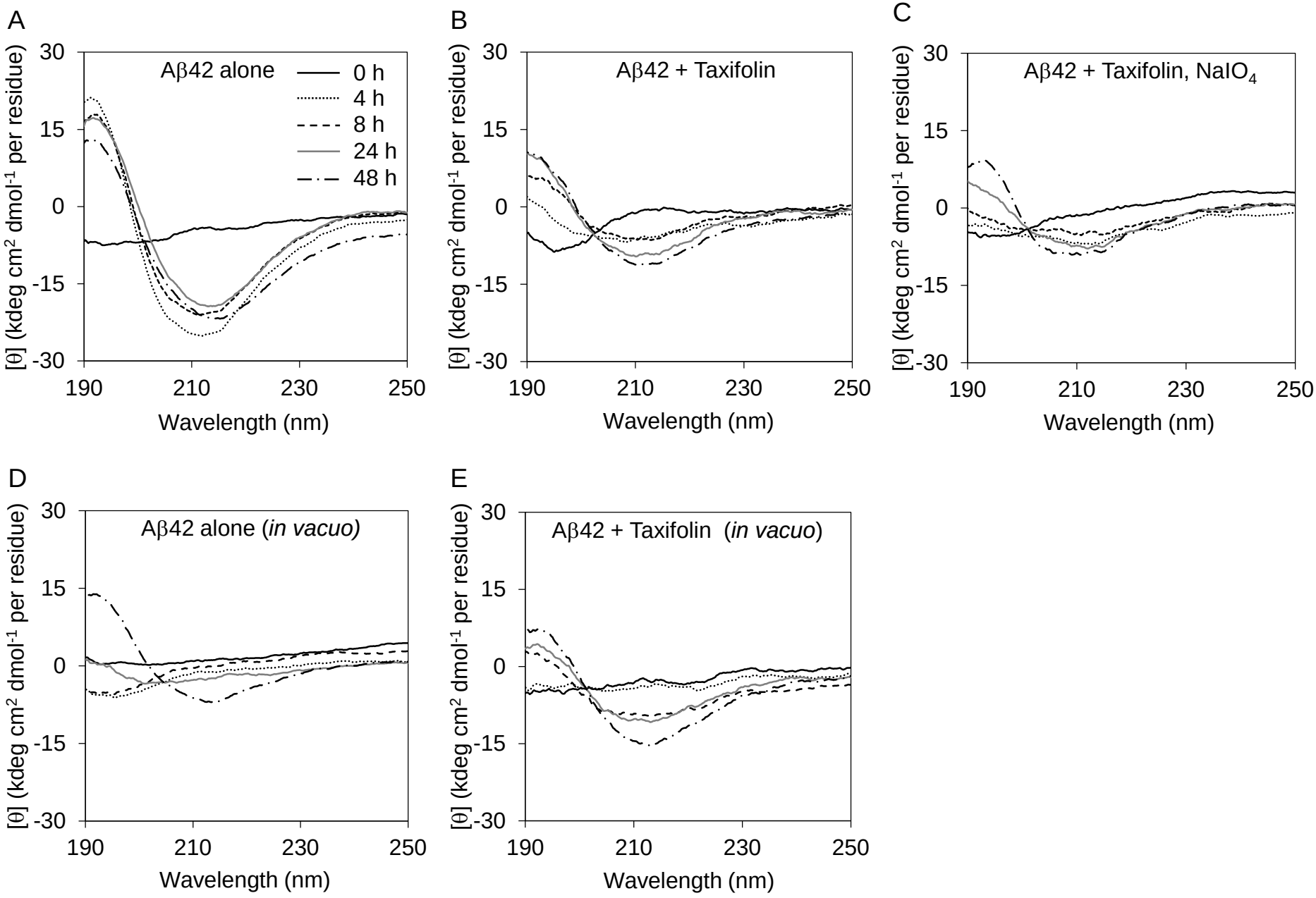
A
Aβ42 alone
0 h
4 h
8 h
24 h
48 h
[θ] (kdeg cm2 dmol-1 per residue)
Wavelength (nm)
B
Aβ42 + Taxifolin
C
Aβ42 + Taxifolin, NaIO4
D
Aβ42 alone (in vacuo)
E
Aβ42 + Taxifolin (in vacuo)

Figure 4

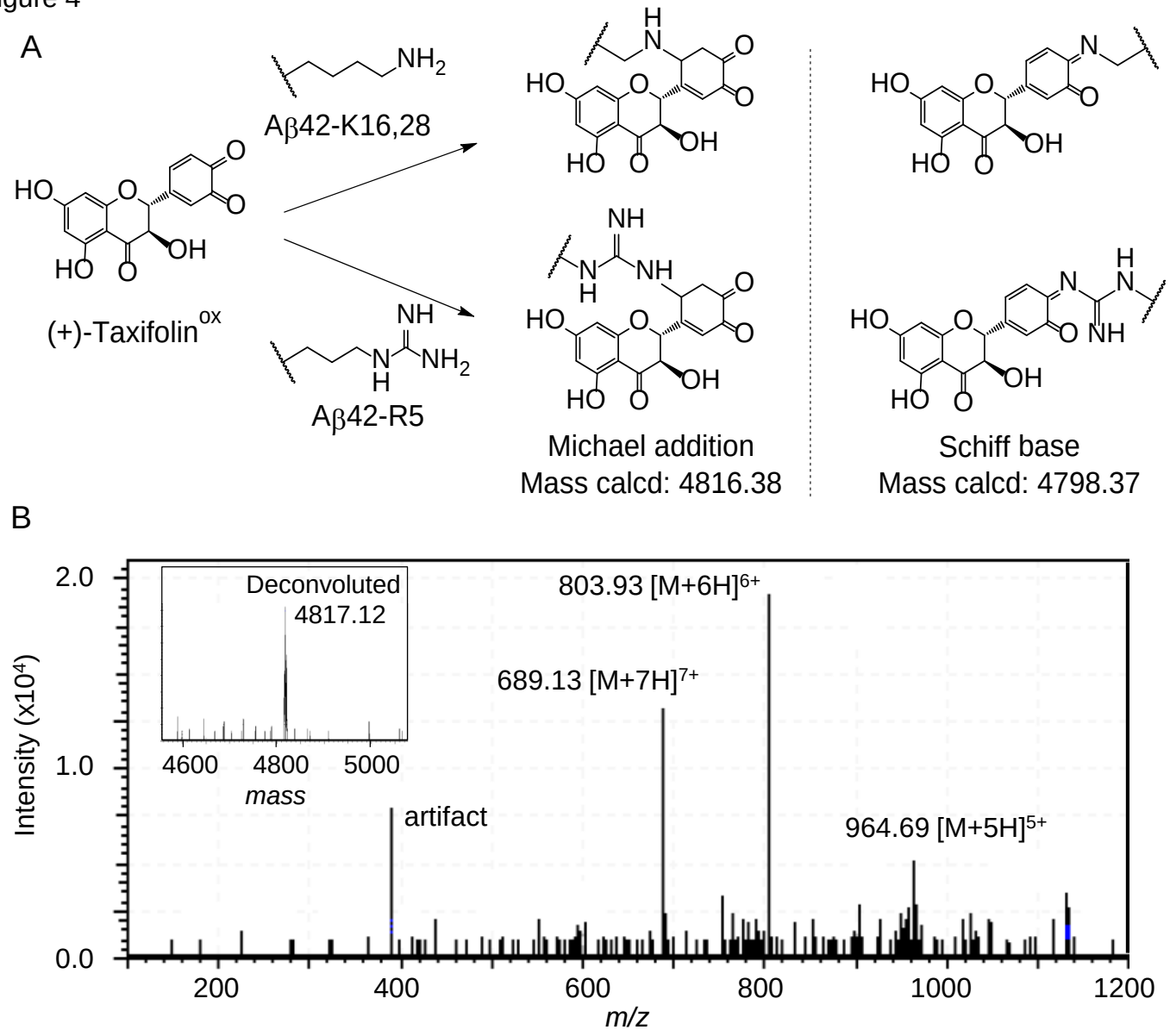
A
Aβ42-K16,28
(+)-Taxifolin^ox
Aβ42-R5
Michael addition
Mass calcd: 4816.38
Schiff base
Mass calcd: 4798.37
B
Deconvoluted
4817.12
4600
4800
5000
mass
803.93 [M+6H]6+
689.13 [M+7H]7+
964.69 [M+5H]5+
artifact
Intensity (x10^4)
2.0
1.0
0.0
200
400
600
800
1000
1200
m/z

Figure 5

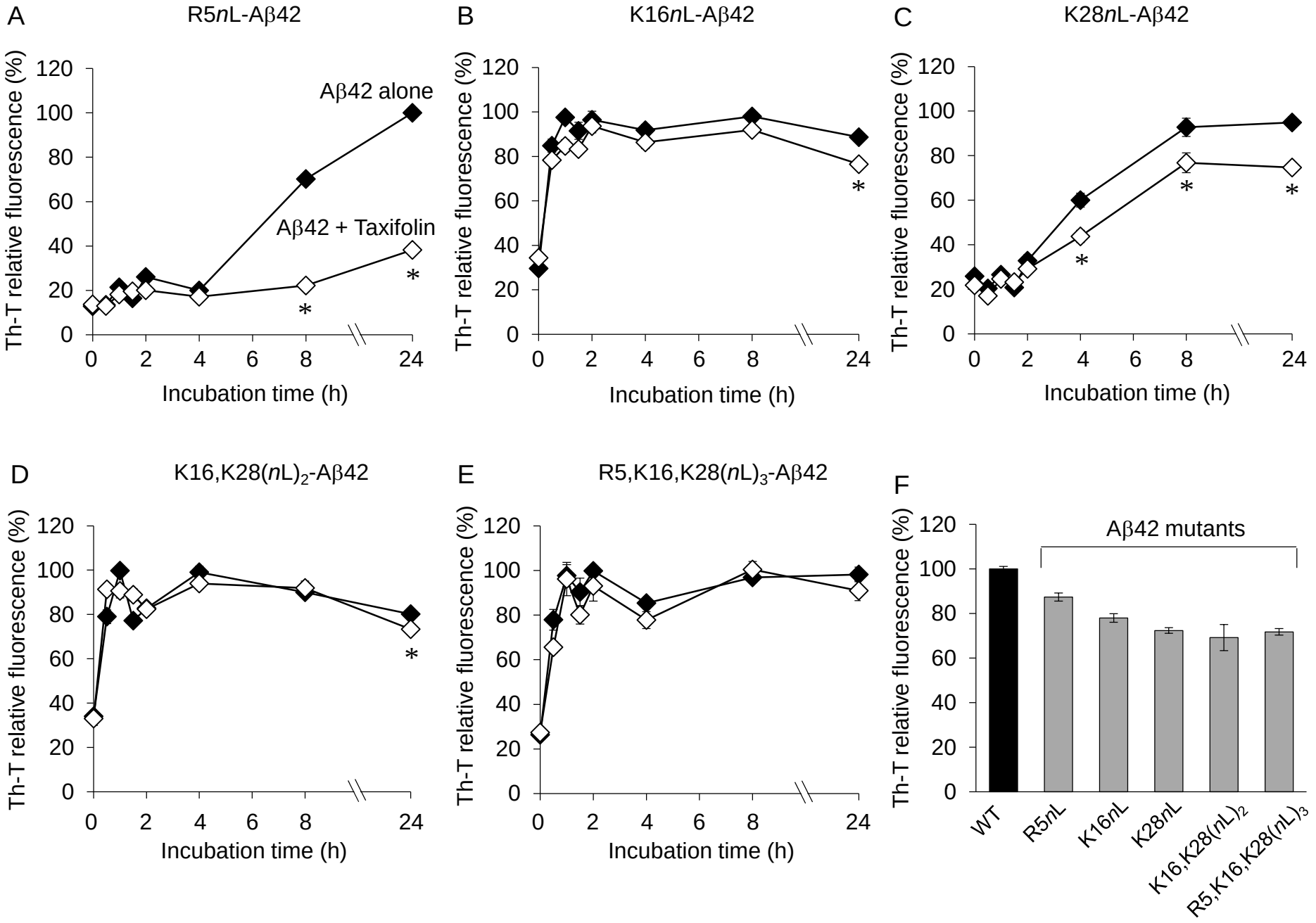
A
R5nL-Aβ42
Aβ42 alone
Aβ42 + Taxifolin
Th-T relative fluorescence (%)
Incubation time (h)
B
K16nL-Aβ42
C
K28nL-Aβ42
D
K16,K28(nL)2-Aβ42
E
R5,K16,K28(nL)3-Aβ42
F
Aβ42 mutants
WT
R5nL
K16nL
K28nL
K16,K28(nL)2
R5,K16,K28(nL)3

Figure 6

A

	$(OH)_3$	$(OH)_2$	OH	—
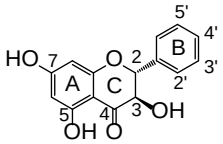 Flavanonol	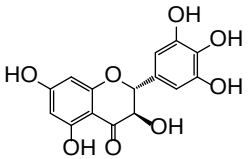 Dihydromyricetin (di*H*-Myr)	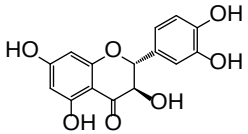 Taxifolin (Tax)	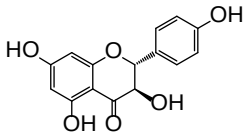 Dihydrokaempferol (di*H*-Kmp)	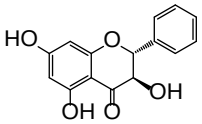 Pinobanksin (Pin)
IC_{50} (μM)	25.3	33.0	>500	>500
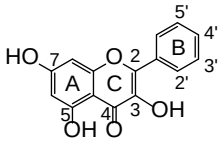 Flavonol	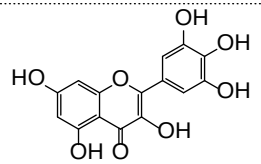 Myricetin (Myr)	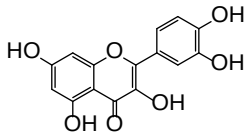 Quercetin (Qur)	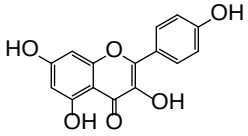 Kaempferol (Kmp)	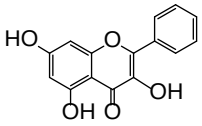 Galangin (Gal)
IC_{50} (μM)	15.1	15.3	75.1	>500
		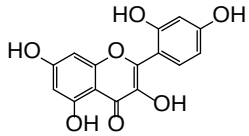 Morin (Mor)	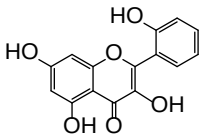 Datiscetin (Dat)	
		30.3	55.4	

B

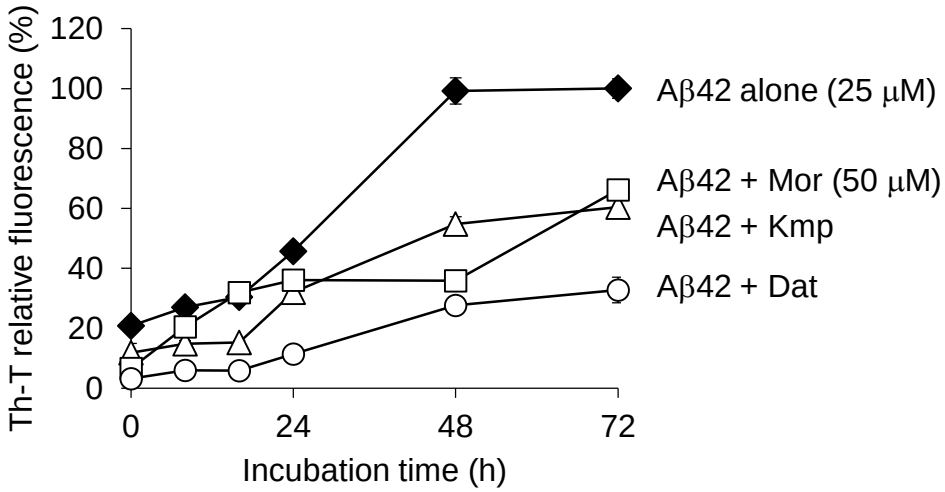

Figure 7

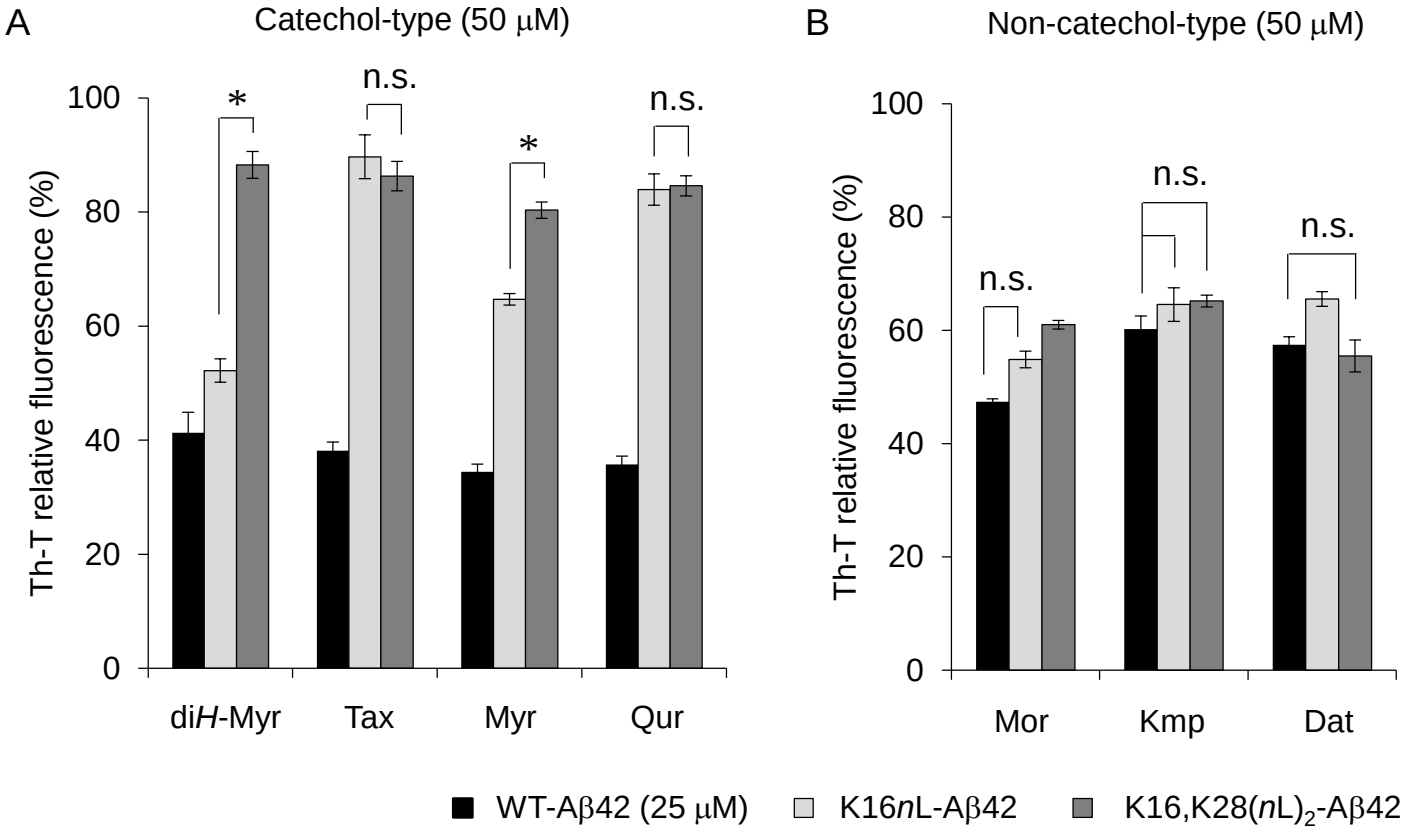
A
Catechol-type (50 μM)
B
Non-catechol-type (50 μM)
Th-T relative fluorescence (%)
100
80
60
40
20
0
*
n.s.
*
n.s.
n.s.
n.s.
n.s.
diH-Myr
Tax
Myr
Qur
Mor
Kmp
Dat
WT-Aβ42 (25 μM)
K16nL-Aβ42
K16,K28(nL)2-Aβ42

Figure 8

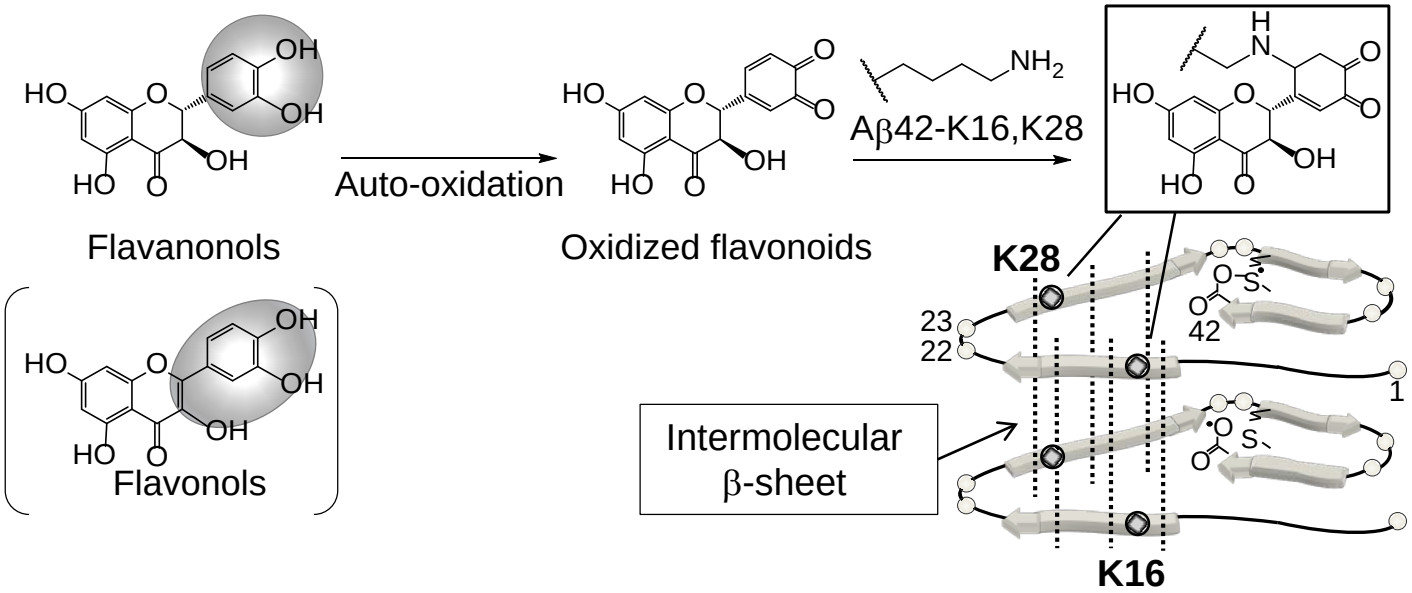
Flavanonols
Auto-oxidation
Oxidized flavonoids
Aβ42-K16,K28
Flavonols
K28
K16
23
22
42
1
Intermolecular
β-sheet

Supplemental Data

Site-specific Inhibitory Mechanism for Aβ42 Aggregation by Catechol-Type Flavonoids Targeting the Lys-Residues*

Mizuho Sato[1], Kazuma Murakami[1], Mayumi Uno[1], Yu Nakagawa[1,2], Sumie Katayama[3], Ken-ichi Akagi[3], Yuichi Masuda[4,5], Kiyonori Takegoshi[4], and Kazuhiro Irie[1]

From [1]Division of Food Science and Biotechnology, Graduate School of Agriculture, Kyoto University, Kyoto 606-8502, Japan
[2]Synthetic Cellular Chemistry Laboratory, RIKEN Advanced Science Institute, Saitama 351-0198, Japan
[3]National Institute of Biomedical Innovation, Osaka 567-0085, Japan
[4]Department of Chemistry, Graduate School of Science, Kyoto University, Kyoto 606-8502, Japan
[5]Graduate School of Pharmaceutical Sciences, Tohoku University, Sendai 980-8578, Japan

*Running title: *Inhibitory Mechanisms of Aβ42 aggregation by Flavonoids*

To whom correspondence should be addressed: Kazuhiro Irie, Ph.D., Kitashirakawa Oiwake-cho, Sakyo-ku, Kyoto 606-8502, Japan. Tel: +81-75-753-6281; Fax: +81-75-753-6284; e-mail: irie@kais.kyoto-u.ac.jp

[Contents]

Scheme S1

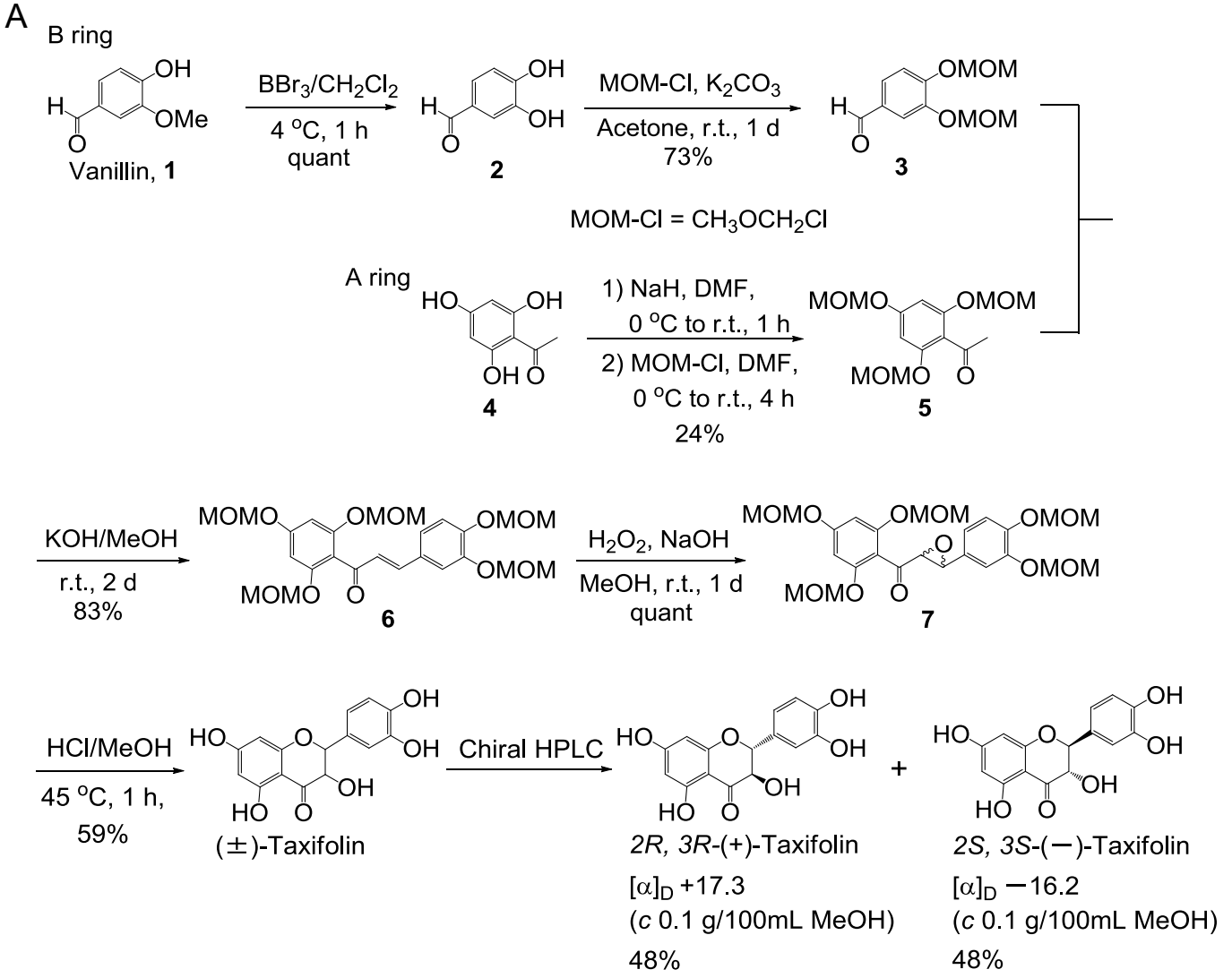
A
B ring
Vanillin, 1
BBr3/CH2Cl2
4 °C, 1 h
quant
2
MOM-Cl, K2CO3
Acetone, r.t., 1 d
73%
3
MOM-Cl = CH3OCH2Cl
A ring
4
1) NaH, DMF,
0 °C to r.t., 1 h
2) MOM-Cl, DMF,
0 °C to r.t., 4 h
24%
5
KOH/MeOH
r.t., 2 d
83%
6
H2O2, NaOH
MeOH, r.t., 1 d
quant
7
HCl/MeOH
45 °C, 1 h,
59%
(±)-Taxifolin
Chiral HPLC
2R, 3R-(+)-Taxifolin
[α]D +17.3
(c 0.1 g/100mL MeOH)
48%
+
2S, 3S-(−)-Taxifolin
[α]D −16.2
(c 0.1 g/100mL MeOH)
48%

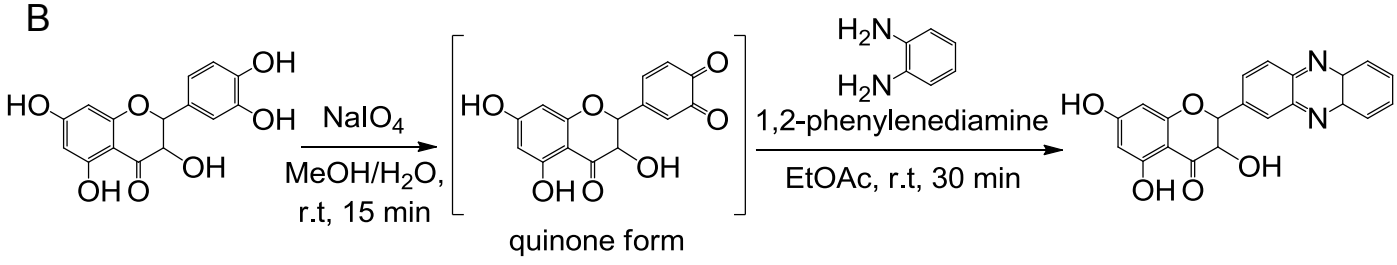
B
NaIO4
MeOH/H2O,
r.t, 15 min
quinone form
1,2-phenylenediamine
EtOAc, r.t, 30 min

Figure S1

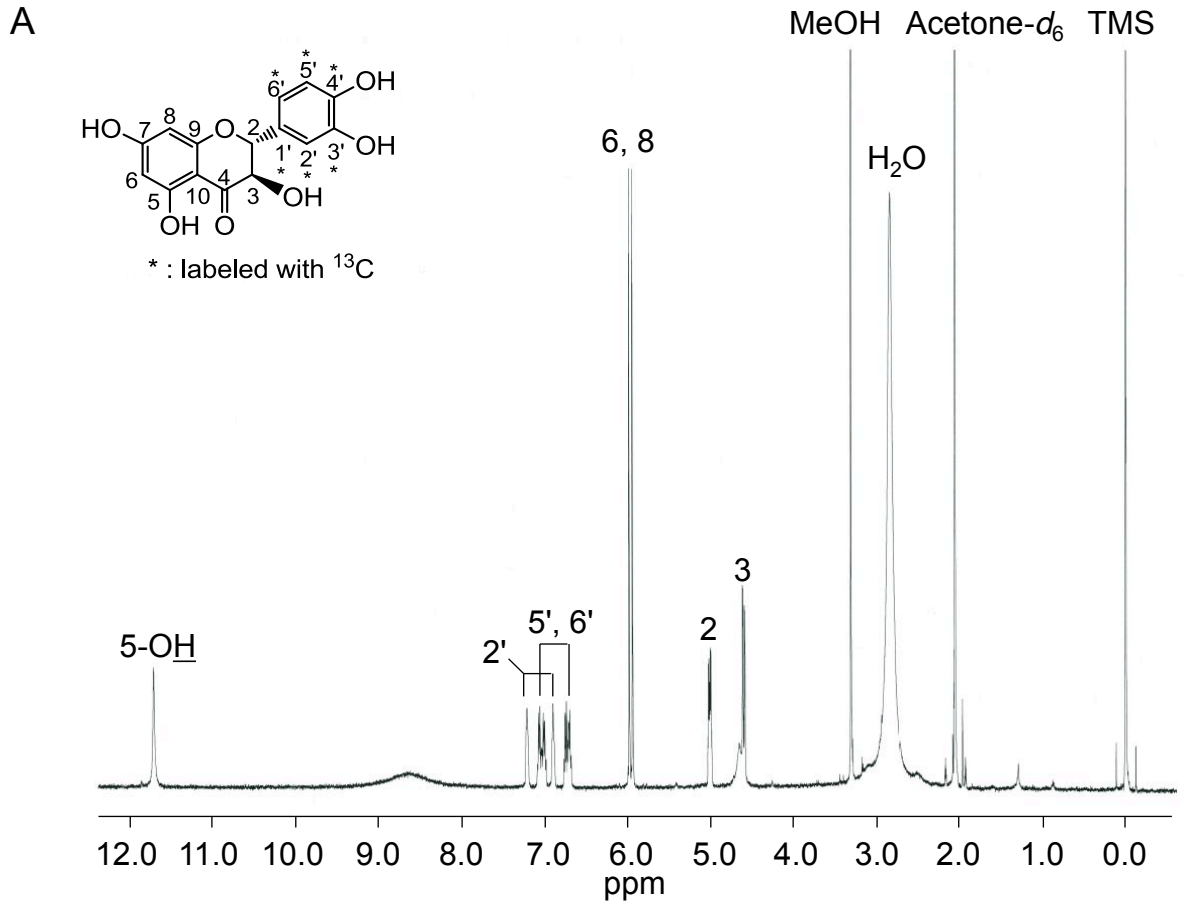
A
MeOH
Acetone-d_6
TMS
6, 8
H_2O
3
2
5', 6'
2'
5-OH
12.0 11.0 10.0 9.0 8.0 7.0 6.0 5.0 4.0 3.0 2.0 1.0 0.0
ppm
* : labeled with ^{13}C

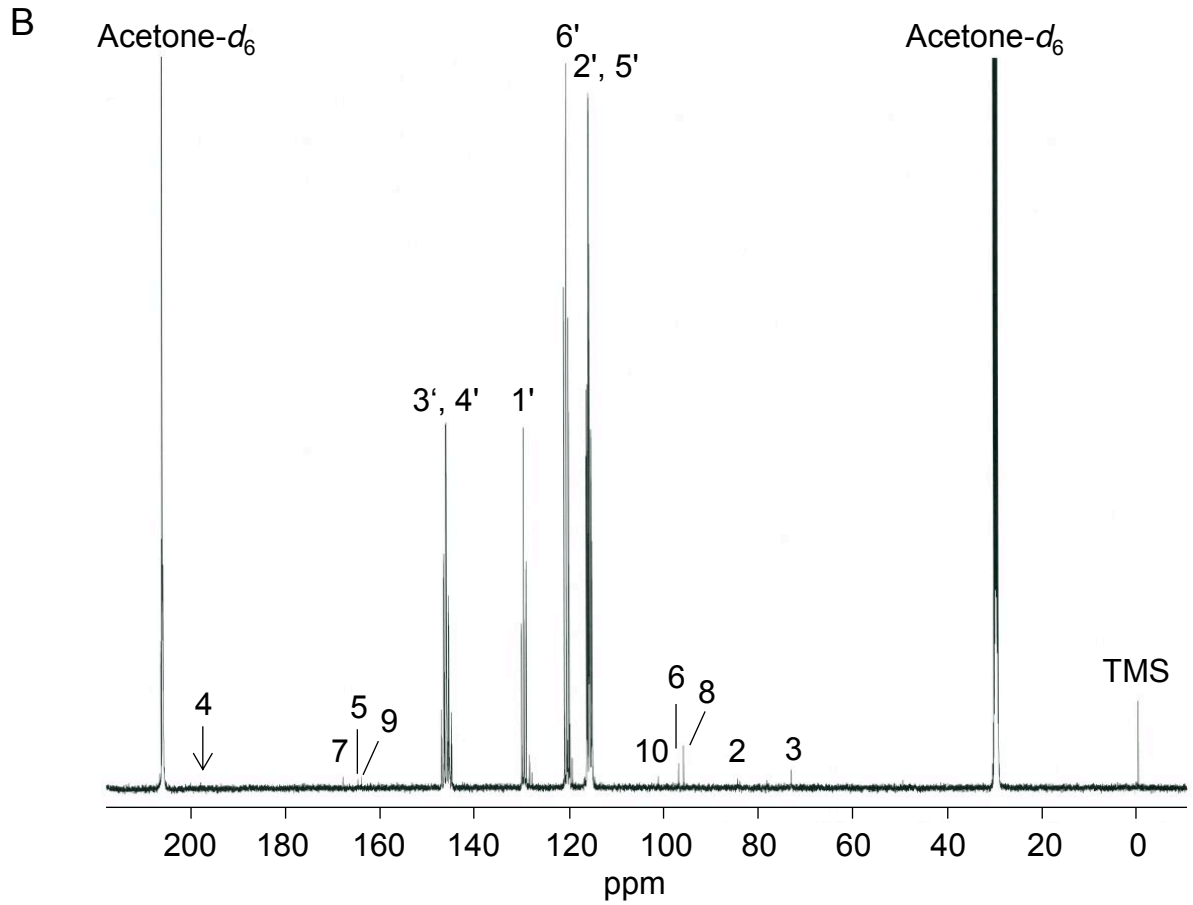
B
Acetone-d_6
6'
2', 5'
Acetone-d_6
3', 4'
1'
4
5
9
7
6
8
10
2
3
TMS
200 180 160 140 120 100 80 60 40 20 0
ppm

Figure S2

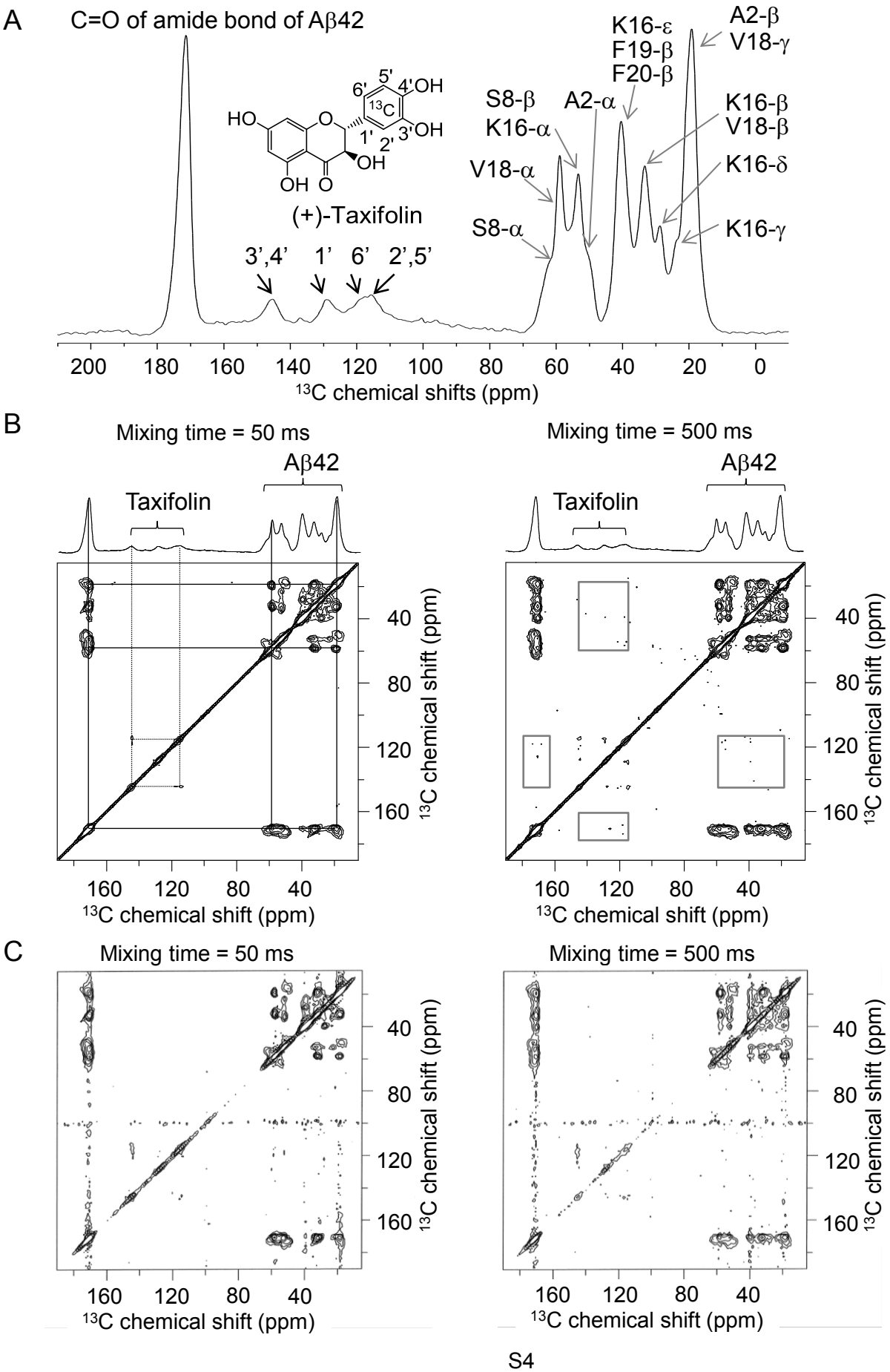
A
C=O of amide bond of Aβ42
(+)-Taxifolin
3',4'
1'
6'
2',5'
S8-α
V18-α
S8-β
K16-α
A2-α
K16-ε
F19-β
F20-β
A2-β
V18-γ
K16-β
V18-β
K16-δ
K16-γ
200 180 160 140 120 100 80 60 40 20 0
13C chemical shifts (ppm)
B
Mixing time = 50 ms
Mixing time = 500 ms
Aβ42
Taxifolin
13C chemical shift (ppm)
C
Mixing time = 50 ms
Mixing time = 500 ms
13C chemical shift (ppm)